Part III

Equations of Motion

Chapter 7

Equations of motion (barotropic component)

MRI.COM predicts the barotropic and baroclinic components (modes) of the equation of motion separately using mode splitting (Sec. 2.2.2). In this chapter, we explain how to solve the barotropic component under the free-surface condtion with z^* vertical coordinate. This chapter contains an overview of mode splitting (Sec. 7.1), the governing equation of the barotropic model (Sec. 7.2), numerical solving techniques of the model (Sec. 7.3), prognostification of the state variables at the baroclinic time step (Sec. 7.4), and the time weighting factor (Sec. 7.5). In addition, a description of optional horizontal diffusion of sea surface height (Sec. 7.6) and a discussion about the effects of mode splitting on the equation of motion (Sec. 7.7) are included as appendices. Finally, we will briefly explain how to set the model (Sec. 7.8). The basic formulation in this chapter is the same as MRI.COMv4, though the representation of the time difference was partially changed with the introduction of the LFAM3 scheme in MRI.COMv5 (Sec. 4.3). See Chapter 6 of the MRI.COMv4 manual for barotropic models that were once used.

7.1 Overview of mode splitting

Before presenting the formulation of the barotropic model, an overview of the mode splitting process in MRI.COM is given. Figure 7.1 presents schematics of the time integration of the barotropic mode and the relation with the baroclinic mode. When the time integration of the baroclinic mode is performed from step n ($t = t_n$) to step $n+1$ ($t = t_{n+1} = t_n + \Delta t_{\mathrm{cl}}$), the corresponding time integration of the barotropic mode is carried out from step n to a step sometime beyond step $n+2$ with the barotropic time interval Δt_{tr} using the vertically integrated forcings (X, Y) at $t = t_n$ calculated in the program that solves the baroclinic mode. A weighted average of the barotropic mode over the integration period is used to represent the vertically integrated velocity $\boldsymbol{U}$ at $t = t_{n+1}$. On the other hand, sea level η is predicted from the continuity equation using $\boldsymbol{U}$ at the $n + \frac{1}{2}$ step, instead of the time-weighted average of the barotropic model (See 7.4.1). See Sec. 4.3 for the role of the barotropic model in the overall time integration scheme of MRI.COM.

7.2 Governing equations of the barotropic submodel

As described in Chapter 2, the prognostic variables in the free-surface barotropic model are the surface elevation (η) and the vertically integrated velocity (U and V) given by Eq. (2.66). The prognostic equations are obtained by integrating momentum and continuity equations vertically.

The momentum equations, Eqs. (2.67) and (2.68), are re-written:

$$\frac{\partial U}{\partial t} - fV = -\frac{(\eta + H)}{\rho_0 h_\mu}\frac{\partial (p_a + \rho_0 g\eta)}{\partial \mu} + X, \tag{7.1}$$

$$\frac{\partial V}{\partial t} + fU = -\frac{(\eta + H)}{\rho_0 h_\psi}\frac{\partial (p_a + \rho_0 g\eta)}{\partial \psi} + Y, \tag{7.2}$$

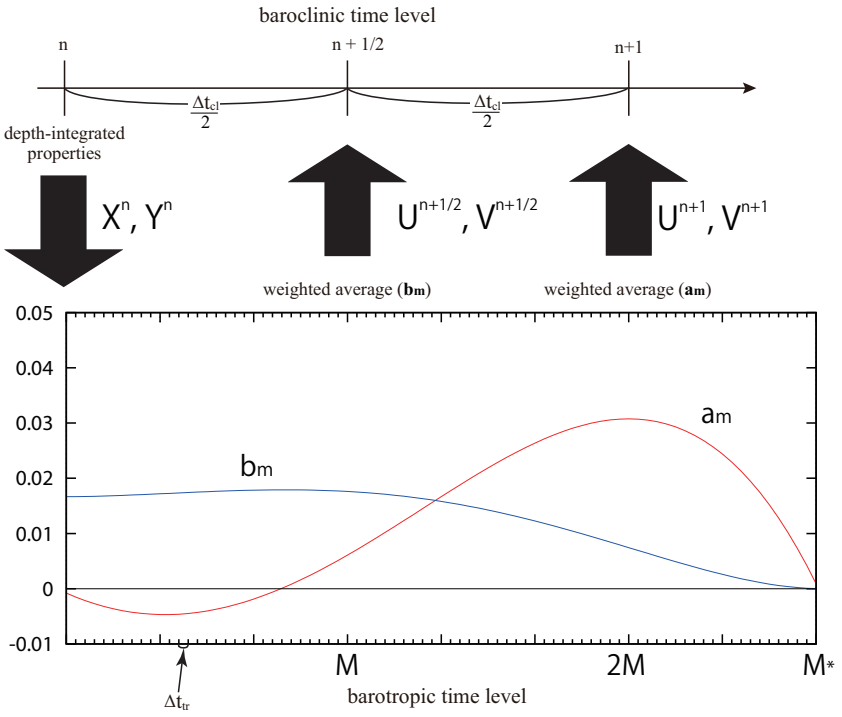

Figure7.1 Schematic figure of the time integration of the barotropic mode and its time-filtering procedure. The weights, a_m and b_m, are for t_{n+1} and $t_{n+\frac{1}{2}}$, respectively.

where

$$
\begin{aligned}
X \equiv \sum_{k=1}^{N} F_\mu = -\nabla_H \cdot \Big(\sum_{k=1}^{N} (\Delta z(u,\ v)u)_{k-\frac{1}{2}} \Big) - \sum_{k=1}^{N} \Big[\frac{v}{h_\mu h_\psi} \Big(\frac{\partial h_\mu}{\partial \psi} u - \frac{\partial h_\psi}{\partial \mu} v \Big) \Big]_{k-\frac{1}{2}} \Delta z_{k-\frac{1}{2}} \\
- \sum_{k=1}^{N} \Big[\frac{1}{\rho_0} \frac{1}{h_\mu} \int_{s_{k-\frac{1}{2}}}^{0} z_s g \rho_\mu ds' \Big] \Delta z_{k-\frac{1}{2}} - \frac{g}{\rho_0 h_\mu} \sum_{k=1}^{N} \big[\rho' z_\mu \big] \Delta z_{k-\frac{1}{2}} + \sum_{k=1}^{N} (\Delta z F^{\mu}_{\text{horz}})_{k-\frac{1}{2}} + F^{\mu}_{\text{surf}} \Delta z_{\frac{1}{2}} + F^{\mu}_{\text{bottom}} \Delta z_{N-\frac{1}{2}} \qquad (7.3)
\end{aligned}
$$

$$
\begin{aligned}
Y \equiv \sum_{k=1}^{N} F_\psi = -\nabla_H \cdot \Big(\sum_{k=1}^{N} (\Delta z(u,\ v)v)_{k-\frac{1}{2}} \Big) + \sum_{k=1}^{N} \Big[\frac{u}{h_\mu h_\psi} \Big(\frac{\partial h_\mu}{\partial \psi} u - \frac{\partial h_\psi}{\partial \mu} v \Big) \Big]_{k-\frac{1}{2}} \Delta z_{k-\frac{1}{2}} \\
- \sum_{k=1}^{N} \Big[\frac{1}{\rho_0} \frac{1}{h_\psi} \int_{s_{k-\frac{1}{2}}}^{0} z_s g \rho_\psi ds' \Big] \Delta z_{k-\frac{1}{2}} - \frac{g}{\rho_0 h_\psi} \sum_{k=1}^{N} \big[\rho' z_\psi \big] \Delta z_{k-\frac{1}{2}} + \sum_{k=1}^{N} (\Delta z F^{\psi}_{\text{horz}})_{k-\frac{1}{2}} + F^{\psi}_{\text{surf}} \Delta z_{\frac{1}{2}} + F^{\psi}_{\text{bottom}} \Delta z_{N-\frac{1}{2}}. \qquad (7.4)
\end{aligned}
$$

Note that the surface atmospheric pressure p_a is omitted in the remainder of this chapter. In MRI.COM, the surface atmospheric pressure is not included unless explicitly specified by SLP option.

The continuity equation, Eq. (2.71), is re-written:

$$
\frac{\partial \eta}{\partial t} + \frac{1}{h_\mu h_\psi} \left\{ \frac{\partial (h_\psi U)}{\partial \mu} + \frac{\partial (h_\mu V)}{\partial \psi} \right\} = (P - E + R + I), \qquad (7.5)
$$

where P is precipitation (positive downward), E is evaporation (positive upward), R is the river discharge rate (positive into the ocean), and I is the mass exchange with the sea ice model (positive into the ocean).

7.3 Time integration on barotropic time levels

The barotropic model is solved under the governing equations, Eqs. (7.1), (7.2) and (7.5). We adopt the "Euler forward-backward" scheme, which is a stable and economical numerical scheme for linear gravity wave equations without advection

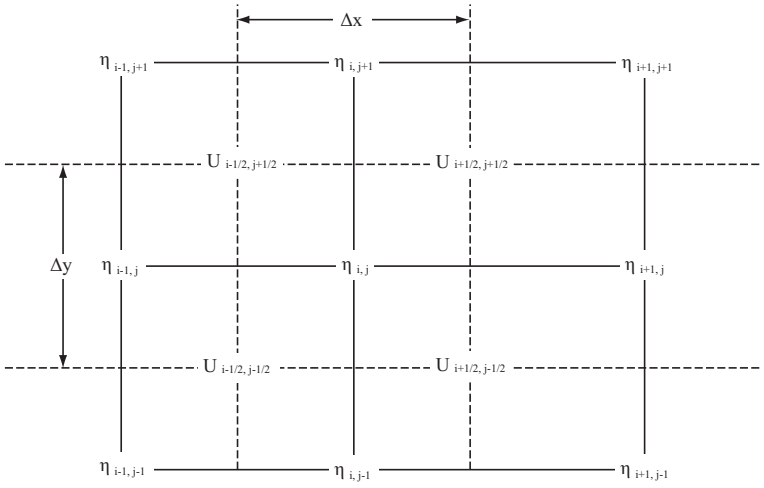

Figure7.2 Grid arrangement of the barotropic model

terms (Mesinger and Arakawa, 1976). This scheme is more stable than the leap-frog scheme. The time step can be doubled for the linear gravity wave equations. In this numerical scheme, either the continuity equation or the momentum equation is calculated first, and then the estimated values are used for calculating the remaining equations. In the procedure of MRI.COM, the surface elevation is first calculated using the continuity equation, Eq. (7.5); the calculated surface elevation is then used to calculate the pressure gradient terms of the momentum equations, Eqs. (7.1) and (7.2). (Killworth et al. (1991) recommended using the Euler backward (Matsuno) scheme for the free surface model except for the tidal problem. The Euler-backward scheme damps higher modes and is more stable. However, the computer burden increases considerably because this scheme calculates the equations twice for one time step. In MRI.COM, stable solutions are efficiently obtained by using the Euler forward-backward scheme because the time filter is applied for the barotropic mode.)

Figure 7.2 illustrates the grid arrangement of the barotropic submodel. The variable η is defined at T-points, and the variables U and V are defined at U-points. Forcing terms (X and Y) in Eqs. (7.1) and (7.2) are calculated in the subroutine for the baroclinic component and defined at U-points.

The finite-difference expression of the continuity equation (Eq. 7.5) is

$$\frac{(\eta'_{i,j}-\eta_{i,j})}{\Delta t_{\rm tr}}+\frac{1}{(h_\mu h_\psi)_{i,j}}\left[(\delta_\mu \overline{h_\psi U}^{\psi})_{i,j}+(\delta_\psi \overline{h_\mu V}^{\mu})_{i,j}\right]=(P-E+R+I)_{i,j}, \tag{7.6}$$

where the subscripts are labeled on the basis of T-points. The variable $\eta_{i,j}$ is located at T-points, and the variables $U_{i+\frac{1}{2},j+\frac{1}{2}}$ and $V_{i+\frac{1}{2},j+\frac{1}{2}}$ are located at U-points. (They are located at $(i+\frac{1}{2}, j+\frac{1}{2})$ on the basis of T-points; see Figure 3.3). The finite-differencing and averaging operators are defined as follows:

$$\begin{aligned}
\delta_\mu A_i &\equiv \frac{A_{i+\frac{1}{2}}-A_{i-\frac{1}{2}}}{\Delta\mu_i}, & \delta_\mu A_{i+\frac{1}{2}} &\equiv \frac{A_{i+1}-A_i}{\Delta\mu_{i+\frac{1}{2}}},\\
\overline{A_i}^{\mu} &\equiv \frac{A_{i+\frac{1}{2}}+A_{i-\frac{1}{2}}}{2}, & \overline{A_{i+\frac{1}{2}}}^{\mu} &\equiv \frac{A_{i+1}+A_i}{2}.
\end{aligned} \tag{7.7}$$

The same applies to ψ. In the program codes, the above equation is multiplied by the area of a T-cell ($\Delta S_{T\,i,j}=(\Delta x\Delta y)_{i,j}=(h_\mu\Delta\mu h_\psi\Delta\psi)_{i,j}$):

$$\begin{aligned}
(\eta'_{i,j}-\eta_{i,j})\Delta S_{T\,i,j}=\Delta t_{\rm tr}\Big\{&(P-E+R+I)_{i,j}\Delta S_{T\,i,j}\\
&-\left(\Delta y_{i+\frac{1}{2},j}\overline{U}^{\psi}_{i+\frac{1}{2},j}-\Delta y_{i-\frac{1}{2},j}\overline{U}^{\psi}_{i-\frac{1}{2},j}\right)-\left(\Delta x_{i,j+\frac{1}{2}}\overline{V}^{\mu}_{i,j+\frac{1}{2}}-\Delta x_{i,j-\frac{1}{2}}\overline{V}^{\mu}_{i,j-\frac{1}{2}}\right)\Big\}.
\end{aligned} \tag{7.8}$$

Averaging operators are defined the same way as the previous ones. This equation is used to obtain the new surface elevation, $\eta'_{i,j}$.

After obtaining $\eta'_{i,j}$, the momentum equations, Eqs. (7.1) and (7.2), are solved. A longer time step can be used when

the semi-implicit scheme is applied for the Coriolis terms in the momentum equations. Their finite-difference forms are

$$\frac{(U'_{i+\frac{1}{2},j+\frac{1}{2}} - U_{i+\frac{1}{2},j+\frac{1}{2}})}{\Delta t_{\rm tr}} - \frac{f(V'_{i+\frac{1}{2},j+\frac{1}{2}} + V_{i+\frac{1}{2},j+\frac{1}{2}})}{2} = -\frac{g(H_{i+\frac{1}{2},j+\frac{1}{2}} + \overline{\overline{\eta'}}^{\mu,\psi}_{i+\frac{1}{2},j+\frac{1}{2}})}{(h_\mu)_{i+\frac{1}{2},j+\frac{1}{2}}}\delta_\mu \overline{\eta'}^{\psi}_{i+\frac{1}{2},j+\frac{1}{2}} + X_{i+\frac{1}{2},j+\frac{1}{2}} \tag{7.9}$$

$$\frac{(V'_{i+\frac{1}{2},j+\frac{1}{2}} - V_{i+\frac{1}{2},j+\frac{1}{2}})}{\Delta t_{\rm tr}} + \frac{f(U'_{i+\frac{1}{2},j+\frac{1}{2}} + U_{i+\frac{1}{2},j+\frac{1}{2}})}{2} = -\frac{g(H_{i+\frac{1}{2},j+\frac{1}{2}} + \overline{\overline{\eta'}}^{\mu,\psi}_{i+\frac{1}{2},j+\frac{1}{2}})}{(h_\psi)_{i+\frac{1}{2},j+\frac{1}{2}}}\delta_\psi \overline{\eta'}^{\mu}_{i+\frac{1}{2},j+\frac{1}{2}} + Y_{i+\frac{1}{2},j+\frac{1}{2}}. \tag{7.10}$$

Next, we solve these equations for $U'_{i+\frac{1}{2},j+\frac{1}{2}}$ and $V'_{i+\frac{1}{2},j+\frac{1}{2}}$. Let the r.h.s. of the above equations be GX and GY. Multiplying both sides by $\Delta t_{\rm tr}$, we have

$$(U'_{i+\frac{1}{2},j+\frac{1}{2}} - U_{i+\frac{1}{2},j+\frac{1}{2}}) - \frac{f\Delta t_{\rm tr}}{2}(V'_{i+\frac{1}{2},j+\frac{1}{2}} + V_{i+\frac{1}{2},j+\frac{1}{2}}) = \Delta t_{\rm tr} GX_{i+\frac{1}{2},j+\frac{1}{2}}, \tag{7.11}$$

$$(V'_{i+\frac{1}{2},j+\frac{1}{2}} - V_{i+\frac{1}{2},j+\frac{1}{2}}) + \frac{f\Delta t_{\rm tr}}{2}(U'_{i+\frac{1}{2},j+\frac{1}{2}} + U_{i+\frac{1}{2},j+\frac{1}{2}}) = \Delta t_{\rm tr} GY_{i+\frac{1}{2},j+\frac{1}{2}}, \tag{7.12}$$

leading to

$$U'_{i+\frac{1}{2},j+\frac{1}{2}} - \frac{f\Delta t_{\rm tr}}{2}V'_{i+\frac{1}{2},j+\frac{1}{2}} = U_{i+\frac{1}{2},j+\frac{1}{2}} + \frac{f\Delta t_{\rm tr}}{2}V_{i+\frac{1}{2},j+\frac{1}{2}} + \Delta t_{\rm tr} GX_{i+\frac{1}{2},j+\frac{1}{2}}, \tag{7.13}$$

$$V'_{i+\frac{1}{2},j+\frac{1}{2}} + \frac{f\Delta t_{\rm tr}}{2}U'_{i+\frac{1}{2},j+\frac{1}{2}} = V_{i+\frac{1}{2},j+\frac{1}{2}} - \frac{f\Delta t_{\rm tr}}{2}U_{i+\frac{1}{2},j+\frac{1}{2}} + \Delta t_{\rm tr} GY_{i+\frac{1}{2},j+\frac{1}{2}}. \tag{7.14}$$

Letting the r.h.s. of the above equations be RX and RY, we may derive expressions for $U'_{i+\frac{1}{2},j+\frac{1}{2}}$ and $V'_{i+\frac{1}{2},j+\frac{1}{2}}$ as follows:

$$U'_{i+\frac{1}{2},j+\frac{1}{2}} = \left\{RX_{i+\frac{1}{2},j+\frac{1}{2}} + \frac{f\Delta t_{\rm tr}}{2}RY_{i+\frac{1}{2},j+\frac{1}{2}}\right\} \Big/ \left\{1 + \left(\frac{f\Delta t_{\rm tr}}{2}\right)^2\right\}, \tag{7.15}$$

$$V'_{i+\frac{1}{2},j+\frac{1}{2}} = \left\{RY_{i+\frac{1}{2},j+\frac{1}{2}} - \frac{f\Delta t_{\rm tr}}{2}RX_{i+\frac{1}{2},j+\frac{1}{2}}\right\} \Big/ \left\{1 + \left(\frac{f\Delta t_{\rm tr}}{2}\right)^2\right\}. \tag{7.16}$$

In the model, the time evolutions of η, U and V are obtained from $t = t_n$ (the initial value) to the barotropic time level M^* (Fig. 7.1) under the finite difference equations, Eqs. (7.8), (7.15) and (7.16).

7.4 Prognostication of state variables at the baroclinic time level

In the split-explicit method, the state at the next baroclinic time level is obtained by using the solution of the barotropic mode explained in the previous section. To do this, an appropriate time-filtering is necessary. The velocity at the baroclinic time level uses the time-filtered barotropic state as the depth averaged velocity.

7.4.1 Weighted averaging to obtain a barotropic state at the baroclinic time level

The main purpose of solving the barotropic submodel on proceeding from the baroclinic time level of $t = t_n$ is to obtain the barotropic state variables η, U, and V at $t = t_{n+1}$. To achieve this, starting from $t = t_n$, the governing equations of the barotropic submodel are integrated slightly beyond $t = t_{n+1}$ to compute the barotropic state variables as a weighted average of those at barotropic time levels.

First, the barotropic current (U^{n+1}, V^{n+1}) at $t = t_{n+1}$ is calculated by the following weighting average:

$$U^{n+1} = \sum_{m=1}^{M^*} a_m U^m, \quad V^{n+1} = \sum_{m=1}^{M^*} a_m V^m, \tag{7.17}$$

using a time-weighting factor a_m, where U^m and V^m are instantaneous state variables at the barotropic time level $t = t_m$.

On the other hand, the surface height at $t = t_{n+1}$, η^{n+1}, is computed by (7.5) using a central difference scheme as

$$\frac{\eta^{n+1} - \eta^n}{\Delta t_{\rm cl}} = -\nabla \cdot \boldsymbol{U}^{n+\frac{1}{2}} + (P - E + R + I), \tag{7.18}$$

where $\boldsymbol{U}^{n+\frac{1}{2}}$ at time step $n+\frac{1}{2}$ is obtained by the following weighting average:

$$U^{n+\frac{1}{2}} = \sum_{m=1}^{M^*} b_m U^m, \quad V^{n+\frac{1}{2}} = \sum_{m=1}^{M^*} b_m V^m. \tag{7.19}$$

This is to make the surface height equation be consistent with the continuity equations in a vertical column (Leclair and Madec, 2009). The time weighting factors, a_m and b_m, are given in Sec. 7.5.

7.4.2 Update of 3-D state variables at the baroclinic time level

With the surface elevation η at $t = t_{n+1}$, the height of the vertical column and the volume of the grid cells in the column are determined (see Chapter 3). Once the volume is determined, 3D state variables at $t = t_{n+1}$ are obtained. The velocity field is computed as follows:

- A provisional baroclinic velocity field (u'^{n+1}, v'^{n+1}) is computed using the tendency terms computed by the baroclinic module.
- The provisional velocity (u'^{n+1}, v'^{n+1}) is integrated over the whole column and the vertical mean of the provisional velocity is computed.
- The vertical mean velocity is subtracted from the provisional velocity first and the actual mean velocity based on (U^{n+1}, V^{n+1}) is added instead in order to yield the final velocity field (u^{n+1}, v^{n+1}).

As explained in Sec. 7.7, these operations correspond to the expression for the velocity at the $(n+1)$th time step in the tendency term (for example, $u'_{k-1/2} - \overline{u'}^z + \langle u \rangle^{n+1}$ of Eqs. (7.55) and (7.56)).

Because Eq. (7.18) is consistent with the continuity equation for the T-cell, computation of tendency of tracer due to advection is both conservative and constancy preserving. This method guarantees that tracer is conserved both globally and locally.

Note that body forcing for the uppermost layer such as wind-forcing and restoration of temperature and salinity to the prescribed values may act differently for grid cells with different width. The body force for the uppermost layer becomes

$$\left(\frac{\partial u}{\partial t}, \frac{\partial v}{\partial t}\right)\Big|_{k=\frac{1}{2}} = \ldots + \frac{1}{\rho_0}\frac{(\tau_\mu, \tau_\psi)}{\Delta z_{\frac{1}{2}}}, \tag{7.20}$$

where (τ_μ, τ_ψ) are the wind stress at the surface (momentum flux), and $\Delta z_{\frac{1}{2}}$ is the variable thickness of the uppermost layer. Thus, the uppermost layer is more accelerated when this layer is thinner than the standard value.

When the restoring condition is applied at the surface, the corresponding temperature and salinity fluxes are

$$F_z^\theta = -\frac{1}{\gamma_\theta}(\theta - \theta^*)\Delta z_{\frac{1}{2}}, \qquad \left.\frac{\partial \theta}{\partial t}\right|_{k=\frac{1}{2}} = \ldots + \frac{F_z^\theta}{\Delta z_{\frac{1}{2}}}, \tag{7.21}$$

$$F_z^S = -\frac{1}{\gamma_s}(S - S^*)\Delta z_{\frac{1}{2}}, \qquad \left.\frac{\partial S}{\partial t}\right|_{k=\frac{1}{2}} = \ldots + \frac{F_z^S}{\Delta z_{\frac{1}{2}}}. \tag{7.22}$$

Thus, the temperature and salinity are more strongly restored to the prescribed values when this layer is thinner than the standard value.

7.5 Time-average weighting function

From MRI.COM version 4, we use a weighted average for the baroclinic time level, as explained by Shchepetkin and McWilliams (2005). Derivation of the weighting functions, a_m and b_m, for $\boldsymbol{U}$ in Eqs. (7.17) and (7.19), is briefly summarized in this section.

First, a weighting shape function to calculate variables at $t = t_{n+1}$ is denoted with $\{a_m\}$. This must satisfy discrete normalization and centroid conditions,

$$\sum_{m=1}^{M^*} a_m \equiv 1, \quad \sum_{m=1}^{M^*} m a_m \equiv 2M, \tag{7.23}$$

where $2M$ is the ratio between barotropic-baroclinic time step ($2M = \Delta t_{\mathrm{cl}}/\Delta t_{\mathrm{tr}}$), and M^* is the last index at which $a_m > 0$, where $2M \le M^*$. The weighted averaging is designed so that aliasing between barotropic and baroclinic modes is

suppressed as well. With a set of $\{a_m\}$, state variables at the baroclinic time level t_{n+1} is computed by Eq. (7.17) and

$$\eta^{n+1} = \sum_{m=1}^{M^*} a_m \eta^m. \tag{7.24}$$

To be consistent with the continuity equation at baroclinic time levels, the vertically integrated continuity equation must satisfy

$$\frac{\eta^{n+1} - \eta^n}{\Delta t_{\rm cl}} = -\nabla \cdot \mathbf{U}^{n+\frac{1}{2}}. \tag{7.25}$$

The flow field at $t = t_{n+\frac{1}{2}}$ can be determined accordingly. Assuming that the vertically integrated continuity equation is advanced in time as

$$\frac{\eta^{m+1} - \eta^m}{\Delta t_{\rm tr}} = -\nabla \cdot \mathbf{U}^{m+\frac{1}{2}}, \tag{7.26}$$

we may obtain the expression for η^m as

$$\eta^m = \eta^0 - \Delta t_{\rm tr} \sum_{m'=0}^{m-1} \nabla \cdot \mathbf{U}^{m'+\frac{1}{2}}. \tag{7.27}$$

Inserting this into Eq. (7.17) and after some manipulations, which is detailed in Shchepetkin and McWilliams (2005), we have

$$\eta^{n+1} = \eta^0 - \Delta t_{\rm cl} \nabla \cdot \sum_{m'=1}^{M^*} b_{m'} \mathbf{U}^{m'-\frac{1}{2}}, \tag{7.28}$$

where $\eta^0 = \eta^n$ and

$$b_{m'} = \frac{1}{2M} \sum_{m=m'}^{M^*} a_m. \tag{7.29}$$

By comparing Eqs. (7.25) and (7.28), vertically integrated flow field at $t = t_{n+\frac{1}{2}}$ is obtained as

$$U^{n+\frac{1}{2}} = \sum_{m=1}^{M^*} b_m U^{m-\frac{1}{2}}, \quad V^{n+\frac{1}{2}} = \sum_{m=1}^{M^*} b_m V^{m-\frac{1}{2}}. \tag{7.30}$$

We require that a set of $\{b_m\}$ satisfies

$$\sum_{m=1}^{M^*} b_m \equiv 1, \quad \sum_{m=1}^{M^*} m b_m \equiv M, \tag{7.31}$$

as well as Eq. (7.23).

Specific shape of the weighting function (a_m) for $\tau = m/2M$, $(1 \le m \le M^*)$ is given as follows:

$$A(\tau) = A_0 \left\{ \left(\frac{\tau}{\tau_0}\right)^p \left[1 - \left(\frac{\tau}{\tau_0}\right)^q\right] - r\frac{\tau}{\tau_0} \right\}, \tag{7.32}$$

where $p = 2$, $q = 2$, $r = 0.2346283$, and A_0 and τ_0 are chosen to satisfy normalization conditions (7.23) and (7.31) iteratively. The initial guess for A_0 and τ_0 is given as follows:

$$A_0 = 1, \quad \tau_0 = \frac{(p+2)(p+q+2)}{(p+1)(p+q+1)}. \tag{7.33}$$

Approximate shape of $\{a_m\}$ and $\{b_m\}$ are shown by red and blue lines of Figure 7.1.

7.6 Horizontal diffusivity of sea surface height (option)

The null mode, or checkerboard pattern, would appear in the sea surface height field commonly in the Arakawa B-grid models. For the purpose of suppressing this mode, a weak horizontal diffusion of sea surface height may be included in the vertically integrated continuity equation,

$$\frac{\partial \eta}{\partial t} + \frac{1}{h_\mu h_\psi} \left\{ \frac{\partial (h_\psi U)}{\partial \mu} + \frac{\partial (h_\mu V)}{\partial \psi} \right\} = \mathcal{D}(\eta) + (P - E + R + I) \tag{7.34}$$

where $\mathcal{D}$ is the diffusion operator (Chapter 12.9 in Griffies (2004)). The diffusion operator mixes a sea surface height in each direction of the model coordinates with the harmonic scheme. The specific form of the harmonic-type diffusivity is represented as follows:

$$\mathcal{D}(\eta) = \frac{1}{h_\mu h_\psi}\left\{\frac{\partial}{\partial\mu}\left(\frac{h_\psi \kappa_H}{h_\mu}\frac{\partial\eta}{\partial\mu}\right) + \frac{\partial}{\partial\psi}\left(\frac{h_\mu \kappa_H}{h_\psi}\frac{\partial\eta}{\partial\psi}\right)\right\} \tag{7.35}$$

$$= \frac{1}{h_\mu h_\psi}\left\{\frac{\partial h_\psi F_\mu^\eta}{\partial\mu} + \frac{\partial h_\mu F_\psi^\eta}{\partial\psi}\right\} \tag{7.36}$$

where κ_H is the horizontal diffusion coefficients and the diffusive fluxes are represented by

$$\mathbf{F}^\eta = -\left(\frac{\kappa_H}{h_\mu}\frac{\partial\eta}{\partial\mu}, \frac{\kappa_H}{h_\psi}\frac{\partial\eta}{\partial\psi}\right). \tag{7.37}$$

Therefore, continuity equation may be rewritten as follows:

$$\frac{\partial\eta}{\partial t} + \frac{1}{h_\mu h_\psi}\left\{\frac{\partial[h_\psi(U+F_\mu^\eta)]}{\partial\mu} + \frac{\partial[h_\mu(V+F_\psi^\eta)]}{\partial\psi}\right\} = (P-E+R+I). \tag{7.38}$$

If the horizontal diffusivity is non-zero for sea surface height, $U^* = U + F_\mu^\eta$ and $V^* = V + F_\psi^\eta$ are treated as the vertically integrated transport velocity, which are divided by the column height to replace the vertical mean velocity based on (U, V) which have been contained in the 3-D velocity field used to advect momentum and tracers. It should be noted that additional restart files are necessary when horizontal diffusion is applied to SSH. This is because $(F_\mu^\eta, F_\psi^\eta)$ are needed to obtain sea surface height for the new time step. MRI.COM provides namelist `nmlrs_ssh_dflx_x` and `nmlrs_ssh_dflx_y` for this purpose.

7.7 The momentum equation modified by the mode splitting

In this appendix, the discretized momentum equation for the 3-D velocity field under the split-explicit method will be derived. This is to clarify the difference from the one for the 3-D velocity under a normal, fully explicit discretizing method. Let us consider reconstructing the flow field of (7.30) from the momentum equation for the barotropic submodel. In the following, we adopted a simple time stepping scheme (forward scheme) and conceptual notations for representing time levels. Because specific expressions will depend upon the choice of time stepping algorithm, the following equations do not necessarily correspond to the time stepping methods used in the model. But this discrepancy is not essential.

At barotropic time levels, momentum equations are advanced in time as follows:

$$U^{m+1} = U^m + \Delta t_{\rm tr} f V^{m+\frac{1}{2}} - \Delta t_{\rm tr}\left[\frac{(\eta+H)}{\rho_0 h_\mu}\frac{\partial(p_a+\rho_0 g\eta)}{\partial\mu}\right]^{m+\frac{1}{2}} + \Delta t_{\rm tr} X, \tag{7.39}$$

$$V^{m+1} = V^m - \Delta t_{\rm tr} f U^{m+\frac{1}{2}} - \Delta t_{\rm tr}\left[\frac{(\eta+H)}{\rho_0 h_\psi}\frac{\partial(p_a+\rho_0 g\eta)}{\partial\psi}\right]^{m+\frac{1}{2}} + \Delta t_{\rm tr} Y, \tag{7.40}$$

where $[\cdot]^{m+\frac{1}{2}}$ is an approximate value of $(\cdot)$ at the time level of $m+\frac{1}{2}$, which is dependent on the choice of the time stepping scheme.

Successive summation of (7.39) and (7.40) over $m' = [0, m-1]$ yields

$$U^m = U^0 + \Delta t_{\rm tr}\sum_{m'=0}^{m-1} f V^{m'+\frac{1}{2}} - \Delta t_{\rm tr}\sum_{m'=0}^{m-1}\left[\frac{(\eta+H)}{\rho_0 h_\mu}\frac{\partial(p_a+\rho_0 g\eta)}{\partial\mu}\right]^{m'+\frac{1}{2}} + m\Delta t_{\rm tr} X, \tag{7.41}$$

$$V^m = V^0 - \Delta t_{\rm tr}\sum_{m'=0}^{m-1} f U^{m'+\frac{1}{2}} - \Delta t_{\rm tr}\sum_{m'=0}^{m-1}\left[\frac{(\eta+H)}{\rho_0 h_\psi}\frac{\partial(p_a+\rho_0 g\eta)}{\partial\psi}\right]^{m'+\frac{1}{2}} + m\Delta t_{\rm tr} Y, \tag{7.42}$$

Applying the time averaging procedure of (7.30) yields

$$\langle U\rangle^{n+1} \equiv \sum_{m=1}^{M^*} b_m U^m \tag{7.43}$$

$$= U^0 + \Delta t_{\rm tr}\sum_{m=1}^{M^*}\left[b_m\sum_{m'=1}^{m} fV^{m'-\frac{1}{2}}\right] - \Delta t_{\rm tr}\sum_{m=1}^{M^*}\left\{b_m\sum_{m'=1}^{m}\left[\frac{(\eta+H)}{\rho_0 h_\mu}\frac{\partial(p_a+\rho_0 g\eta)}{\partial\mu}\right]^{m'-\frac{1}{2}}\right\} + \sum_{m=1}^{M^*} m b_m \Delta t_{\rm tr} X, \tag{7.44}$$

$$\langle V\rangle^{n+1} \equiv \sum_{m=1}^{M^*} b_m V^m \tag{7.45}$$

$$= V^0 - \Delta t_{\rm tr}\sum_{m=1}^{M^*}\left[b_m\sum_{m'=1}^{m} fU^{m'-\frac{1}{2}}\right] - \Delta t_{\rm tr}\sum_{m=1}^{M^*}\left\{b_m\sum_{m'=1}^{m}\left[\frac{(\eta+H)}{\rho_0 h_\psi}\frac{\partial(p_a+\rho_0 g\eta)}{\partial\psi}\right]^{m'-\frac{1}{2}}\right\} + \sum_{m=1}^{M^*} m b_m \Delta t_{\rm tr} Y, \tag{7.46}$$

which are rearranged to have a form

$$\langle U\rangle^{n+1} = U^0 + \Delta t_{\rm cl} f\langle\langle V\rangle\rangle^{n+\frac{1}{2}} - \Delta t_{\rm cl}\left\langle\left\langle\frac{(\eta+H)}{\rho_0 h_\mu}\frac{\partial(p_a+\rho_0 g\eta)}{\partial\mu}\right\rangle\right\rangle^{n+\frac{1}{2}} + \Delta t_{\rm cl} X^n, \tag{7.47}$$

$$\langle V\rangle^{n+1} = V^0 - \Delta t_{\rm cl} f\langle\langle U\rangle\rangle^{n+\frac{1}{2}} - \Delta t_{\rm cl}\left\langle\left\langle\frac{(\eta+H)}{\rho_0 h_\psi}\frac{\partial(p_a+\rho_0 g\eta)}{\partial\psi}\right\rangle\right\rangle^{n+\frac{1}{2}} + \Delta t_{\rm cl} Y^n, \tag{7.48}$$

where $\langle\langle\cdot\rangle\rangle^{n+\frac{1}{2}} \equiv \sum_{m=1}^{M^*} b_m \sum_{m'=1}^{m}(\cdot)^{m'-\frac{1}{2}}$.

On the other hand, the baroclinic momentum equation where surface pressure gradient term is dropped is

$$\frac{u'_{k-\frac{1}{2}}\Delta z^{n+1}_{k-\frac{1}{2}} - u^n_{k-\frac{1}{2}}\Delta z^n_{k-\frac{1}{2}}}{\Delta t_{\rm cl}} = f[v_{k-\frac{1}{2}}\Delta z_{k-\frac{1}{2}}]^{n+\frac{1}{2}} + F^n_\mu, \tag{7.49}$$

$$\frac{v'_{k-\frac{1}{2}}\Delta z^{n+1}_{k-\frac{1}{2}} - v^n_{k-\frac{1}{2}}\Delta z^n_{k-\frac{1}{2}}}{\Delta t_{\rm cl}} = -f[u_{k-\frac{1}{2}}\Delta z_{k-\frac{1}{2}}]^{n+\frac{1}{2}} + F^n_\psi. \tag{7.50}$$

This is vertically summed up to give

$$\frac{\sum_{k=1}^{N}(u'_{k-\frac{1}{2}}\Delta z^{n+1}_{k-\frac{1}{2}}) - \sum_{k=1}^{N}(u^n_{k-\frac{1}{2}}\Delta z^n_{k-\frac{1}{2}})}{\Delta t_{\rm cl}} = f\sum_{k=1}^{N}[v_{k-\frac{1}{2}}\Delta z_{k-\frac{1}{2}}]^{n+\frac{1}{2}} + X^n, \tag{7.51}$$

$$\frac{\sum_{k=1}^{N}(v'_{k-\frac{1}{2}}\Delta z^{n+1}_{k-\frac{1}{2}}) - \sum_{k=1}^{N}(v^n_{k-\frac{1}{2}}\Delta z^n_{k-\frac{1}{2}})}{\Delta t_{\rm cl}} = -f\sum_{k=1}^{N}[u_{k-\frac{1}{2}}\Delta z_{k-\frac{1}{2}}]^{n+\frac{1}{2}} + Y^n. \tag{7.52}$$

X^n and Y^n are removed from (7.47), (7.48), (7.51), and (7.52) to give

$$\frac{\sum_{k=1}^{N}(\langle u\rangle^{n+1}\Delta z^{n+1}_{k-\frac{1}{2}}) - \sum_{k=1}^{N}(u'_{k-\frac{1}{2}}\Delta z^{n+1}_{k-\frac{1}{2}})}{\Delta t_{\rm cl}} = f\langle\langle V\rangle\rangle^{n+\frac{1}{2}} - f\sum_{k=1}^{N}[v_{k-\frac{1}{2}}\Delta z_{k-\frac{1}{2}}]^{n+\frac{1}{2}} - \left\langle\left\langle\frac{(\eta+H)}{\rho_0 h_\mu}\frac{\partial(p_a+\rho_0 g\eta)}{\partial\mu}\right\rangle\right\rangle^{n+\frac{1}{2}} \tag{7.53}$$

$$\frac{\sum_{k=1}^{N}(\langle v\rangle^{n+1}\Delta z^{n+1}_{k-\frac{1}{2}}) - \sum_{k=1}^{N}(v'_{k-\frac{1}{2}}\Delta z^{n+1}_{k-\frac{1}{2}})}{\Delta t_{\rm cl}} = -f\langle\langle U\rangle\rangle^{n+\frac{1}{2}} + f\sum_{k=1}^{N}[u_{k-\frac{1}{2}}\Delta z_{k-\frac{1}{2}}]^{n+\frac{1}{2}} - \left\langle\left\langle\frac{(\eta+H)}{\rho_0 h_\psi}\frac{\partial(p_a+\rho_0 g\eta)}{\partial\psi}\right\rangle\right\rangle^{n+\frac{1}{2}}. \tag{7.54}$$

This is combined with (7.49) and (7.50) to give

$$\frac{\left(u'_{k-\frac{1}{2}} - \overline{u'}^{z} + \langle u\rangle^{n+1}\right)\Delta z^{n+1}_{k-\frac{1}{2}} - u^{n}_{k-\frac{1}{2}}\Delta z^{n}_{k-\frac{1}{2}}}{\Delta t_{\mathrm{cl}}} = f\left[v_{k-\frac{1}{2}}\Delta z_{k-\frac{1}{2}}\right]^{n+\frac{1}{2}} - f\overline{[v]^{n+\frac{1}{2}}}^{z}\Delta z^{n+1}_{k-\frac{1}{2}} + f\langle\langle v\rangle\rangle^{n+\frac{1}{2}}\Delta z^{n+1}_{k-\frac{1}{2}} - \frac{\Delta z^{n+1}_{k-\frac{1}{2}}}{\eta^{n+1}+H}\left\langle\left\langle\frac{(\eta+H)}{\rho_0 h_\mu}\frac{\partial(p_a+\rho_0 g\eta)}{\partial\mu}\right\rangle\right\rangle^{n+\frac{1}{2}} + F^{n}_{\mu} \tag{7.55}$$

$$\frac{\left(v'_{k-\frac{1}{2}} - \overline{v'}^{z} + \langle v\rangle^{n+1}\right)\Delta z^{n+1}_{k-\frac{1}{2}} - v^{n}_{k-\frac{1}{2}}\Delta z^{n}_{k-\frac{1}{2}}}{\Delta t_{\mathrm{cl}}} = -f\left[u_{k-\frac{1}{2}}\Delta z_{k-\frac{1}{2}}\right]^{n+\frac{1}{2}} + f\overline{[u]^{n+\frac{1}{2}}}^{z}\Delta z^{n+1}_{k-\frac{1}{2}} - f\langle\langle u\rangle\rangle^{n+\frac{1}{2}}\Delta z^{n+1}_{k-\frac{1}{2}} - \frac{\Delta z^{n+1}_{k-\frac{1}{2}}}{\eta^{n+1}+H}\left\langle\left\langle\frac{(\eta+H)}{\rho_0 h_\psi}\frac{\partial(p_a+\rho_0 g\eta)}{\partial\psi}\right\rangle\right\rangle^{n+\frac{1}{2}} + F^{n}_{\psi}, \tag{7.56}$$

where $\overline{(\ldots)}^{z}$ denotes the thickness weighted vertical average. This is the momentum balance for the total velocity field under the mode-splitting scheme. In comparison with (7.49) and (7.50), the correction terms appear in the tendency and Coriolis terms owing to the use of the split-explicit method. In the tendency term on the l.h.s., the vertically averaged velocity $(\overline{u'}^{z}, \overline{v'}^{z})$ is replaced by the prediction of the barotropic model $(\langle u\rangle^{n+1}, \langle v\rangle^{n+1})$. Likewise on the r.h.s., the Coriolis term takes a form in which vertical average for $[\mathbf{u}_{k+\frac{1}{2}}]^{n+\frac{1}{2}}$ is replaced by $\langle\langle\mathbf{u}\rangle\rangle^{n+\frac{1}{2}}$.

7.8 Usage

Behavior of the barotropic model at run time is specified by the three namelist blocks shown on Tables 7.1 through 7.3. For the initial condition of the model, restart files must be prepared for five variables: sea surface height, X- and Y-ward barotropic transports, and X- and Y-ward transports due to SSH diffusion.

In addition, following model options are available.

`SLP`: Sea surface is elevated/depressed according to surface atmospheric pressure
Give atmospheric sea-level pressure, p_a in (7.1) and (7.2), to the model by namelist `nml_force_data` (See Table 14.4).

`FSVISC`: Explicit viscosity is added to the barotropic momentum equation
Specify the horizontal viscosity coefficient by namelist `nml_barotropic_visc_horz`. See Section 7.3 for the time discretization method.

See `docs/README.Namelist` for namelist details.

Table7.1 Namelist `nml_barotropic_model` for the specifying basic features of the barotropic model (see Section 7.8)

variable	units	description	usage
`dt_barotropic_sec`	sec	time step interval	required

Table7.2 Namelist `nml_barotropic_run` for starting the barotropic model (see Section 7.8)

variable	units	description	usage
`l_rst_barotropic_in`	logical	read initial restart for sea surface and transport or not	default = `l_rst_in`
`l_rst_barotropic_dflx_in`	logical	read initial restart for diffusive flux of SSH or not (Section 7.6)	default = `l_rst_barotropic_in`

Table7.3 Namelist `nml_barotropic_diff` for specifying SSH diffusion (see Section 7.8)

variable	units	description	usage
`ssh_diff_cm2ps`	$\mathrm{cm^2\ s^{-1}}$	diffusivity for SSH (Section 7.6)	default = zero

Chapter 8

Equations of motion (baroclinic component)

This chapter explains how to solve the baroclinic momentum equations (2.76) and (2.77), which are re-written:

$$\begin{aligned}
&\frac{\partial(z_s u)}{\partial t}+\frac{1}{h_\mu h_\psi}\left\{\frac{\partial(z_s h_\psi uu)}{\partial\mu}+\frac{\partial(z_s h_\mu vu)}{\partial\psi}\right\}+\frac{\partial(z_s\dot{s}u)}{\partial s}+z_s\frac{v}{h_\mu h_\psi}\left(\frac{\partial h_\mu}{\partial\psi}u-\frac{\partial h_\psi}{\partial\mu}v\right)-z_s f v\\
&\quad=-z_s\frac{1}{\rho_0 h_\mu}\frac{\partial}{\partial\mu}\left(g\int_{z(z^*)}^{\eta}\rho' dz\right)-z_s\frac{g\rho'}{\rho_0 h_\mu}\frac{\partial z}{\partial\mu}\\
&\qquad+z_s\frac{1}{\rho_0}(\nabla\cdot\tau_{\text{horizontal strain}})_u+z_s\frac{1}{z_s}\frac{\partial}{\partial s}\left(\frac{\nu_V}{z_s}\frac{\partial u}{\partial s}\right),
\end{aligned}\tag{8.1}$$

$$\begin{aligned}
&\frac{\partial(z_s v)}{\partial t}+\frac{1}{h_\mu h_\psi}\left\{\frac{\partial(z_s h_\psi uv)}{\partial\mu}+\frac{\partial(z_s h_\mu vv)}{\partial\psi}\right\}+\frac{\partial(z_s\dot{s}v)}{\partial s}+z_s\frac{u}{h_\mu h_\psi}\left(\frac{\partial h_\psi}{\partial\mu}v-\frac{\partial h_\mu}{\partial\psi}u\right)+z_s f u\\
&\quad=-z_s\frac{1}{\rho_0 h_\psi}\frac{\partial}{\partial\psi}\left(g\int_{z(z^*)}^{\eta}\rho' dz\right)-z_s\frac{g\rho'}{\rho_0 h_\psi}\frac{\partial z}{\partial\psi}\\
&\qquad+z_s\frac{1}{\rho_0}(\nabla\cdot\tau_{\text{horizontal strain}})_v,+z_s\frac{1}{z_s}\frac{\partial}{\partial s}\left(\frac{\nu_V}{z_s}\frac{\partial v}{\partial s}\right).
\end{aligned}\tag{8.2}$$

The advection terms are explained in Section 8.1, the pressure gradient terms in Section 8.2, the viscosity terms in Section 8.3 and the Coriolis terms in Section 8.4. Finally, Section 8.5 explains usage. The purpose of this chapter is to find the temporary velocity (u', v') shown by Eqs. (2.78) and (2.79). See Section 2.2.2 for the procedure to obtain the absolute velocity (u, v) based on (u', v').

One of the unique characteristics of MRI.COM's momentum advection terms is that there are oblique exchanges of momentum between U-cells that share only a corner. This scheme enables the flow field around and over the bottom topography to be naturally expressed. Furthermore, quasi-enstrophies, $(\partial u/\partial y)^2$ and $(\partial v/\partial x)^2$, for the U-cells away from land are conserved in calculating the momentum advection for horizontally non-divergent flows. The description of momentum advection in Section 8.1 is based on Ishizaki and Motoi (1999).

The discrete expressions for the viscosity terms in the momentum equations are based on generalized orthogonal coordinates. A harmonic operator is used as the default assuming a no-slip condition on the land-sea boundaries. A biharmonic operator (`VISBIHARM` option) and a parameterization of viscosity as a function of deformation rate (`SMAGOR` option) may also be used.

8.1 Advection terms

Chapter 6 demonstrated that the mass fluxes used for calculating momentum advection are identical to those for the mass continuity of the U-cell, and that they are obtained by an averaging operation (6.20) of those for the T-cell mass continuity (6.21). This is the preliminaries for constructing the general mass flux form over an arbitrary bottom and coastal topography. Its vertical part can express diagonally upward mass fluxes over bottom relief and its horizontal part can express horizontally diagonal mass fluxes along coast lines (Ishizaki and Motoi, 1999).

Here we explain how to obtain the mass fluxes used in the momentum advection and how to get the finite difference expression of the advection terms.

The horizontal subscript indices of variables are integers for the T-point (i, j), and therefore, $(i+\frac{1}{2}, j+\frac{1}{2})$ for the U-point. In the vertical direction, integer k is used for the level of the vertical mass fluxes and the level for the T- and U-points a half vertical grid size lower is expressed by $k+\frac{1}{2}$ (Figure 3.3(a)).

8.1.1 Vertical mass fluxes and its momentum advection

Following (6.20), the vertical mass flux at the upper surface, level k, of the U-cell $(i+\frac{1}{2}, j+\frac{1}{2}, k+\frac{1}{2})$, $\overline{W}^U_{i+\frac{1}{2},j+\frac{1}{2},k}$, is defined by surrounding W^T as

$$\overline{W}^U_{i+\frac{1}{2},j+\frac{1}{2},k} = \frac{W^T_{i,j,k}}{N_{i,j,k+\frac{1}{2}}} + \frac{W^T_{i+1,j,k}}{N_{i+1,j,k+\frac{1}{2}}} + \frac{W^T_{i,j+1,k}}{N_{i,j+1,k+\frac{1}{2}}} + \frac{W^T_{i+1,j+1,k}}{N_{i+1,j+1,k+\frac{1}{2}}}, \tag{8.3}$$

where $N_{i,j,k+\frac{1}{2}}$ is the number of sea grid cells around the T-point $T_{i,j}$ in layer $k+\frac{1}{2}$.

On the other hand, the vertical mass flux at the bottom surface, level k, of the U-cell $(i+\frac{1}{2}, j+\frac{1}{2}, k-\frac{1}{2})$, $\mathcal{W}^U_{i+\frac{1}{2},j+\frac{1}{2},k}$ is defined as

$$\mathcal{W}^U_{i+\frac{1}{2},j+\frac{1}{2},k} = \frac{W^T_{i,j,k}}{N_{i,j,k-\frac{1}{2}}} + \frac{W^T_{i+1,j,k}}{N_{i+1,j,k-\frac{1}{2}}} + \frac{W^T_{i,j+1,k}}{N_{i,j+1,k-\frac{1}{2}}} + \frac{W^T_{i+1,j+1,k}}{N_{i+1,j+1,k-\frac{1}{2}}}. \tag{8.4}$$

Though W^T are continuous at the boundary of vertically adjacent T-cells, $\overline{W}^U_{i+\frac{1}{2},j+\frac{1}{2},k}$ and $\mathcal{W}^U_{i+\frac{1}{2},j+\frac{1}{2},k}$ seem to be discontinuous at the boundary when N are vertically different, for example, $N_{i,j,k+\frac{1}{2}} < N_{i,j,k-\frac{1}{2}}$, over the bottom relief. However, this apparent discrepancy can be consistently interpreted by introducing diagonally upward or downward mass fluxes as shown below.

a. One-dimensional variation of bottom relief

We first consider a case in which the bottom depth varies in one direction like a staircase and a barotropic current flows from the left to the right over the topography. Figure 8.1(a) indicates the mass continuity for T-cells to conserve barotropy in shallow regions (the U-points are just intermediate between T-points) . Figure 8.1(b) depicts the mass continuity for U-cells, derived from those for adjacent T-cells. Except for fluxes just on the bottom slope, each flux is obtained as a mean value of neighboring fluxes for T-cells. Just on the bottom slope, we must introduce a flux that flows along the slope to ensure mass continuity. The lowermost U-cells at the slope have nonzero vertical flux at the bottom. The barotropy of the flow and the distribution of vertical velocity are thereby kept reasonable for U-cell fluxes.

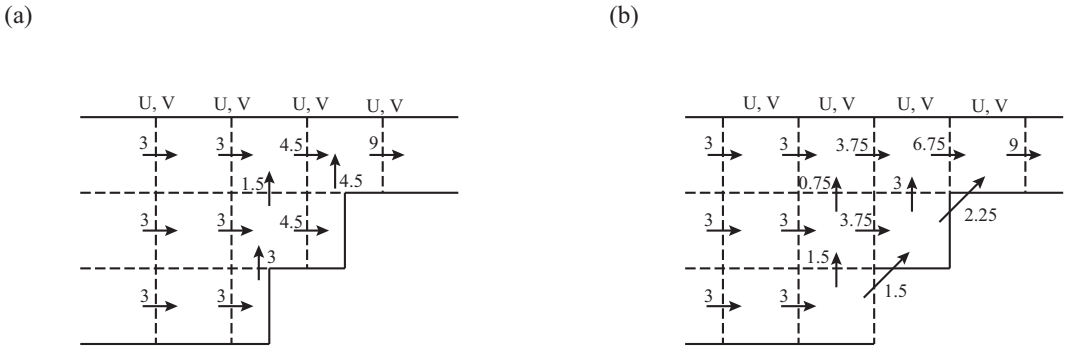

Figure8.1 (a) Two-dimensional mass fluxes for T-cells on a stair-like topography. (b) Two-dimensional mass fluxes for U-cells on the same topography.

b. Two-dimensional variation of bottom depth

The diagonally upward or downward mass fluxes introduced in the previous simple case are generalized for flows over bottom topography that varies two-dimensionally. For simplicity, we consider a two-layer case without losing generality. First, we consider three examples of bottom relief, and then generalize the results.

■Example 1 Consider a case in which all cells are sea cells in the upper and lower layers except for cell **d** in the lower layer (cell $\mathbf{d}_l$) (Figure 8.2). We use suffixes l and u to designate the lower and the upper layer. The central T-point and T-cell are represented by A. The vertical mass flux W^T should be continuous at the interface between cells A_l and A_u, though the area of cell A_l (3/4 measured in grid area units) differs from that of A_u (1 unit). Let us consider how this T-cell mass flux W^T should be distributed to the mass flux W^U of neighboring cells represented by **a**, **b**, **c**, and **d**. In the lower

layer, W_T is shared by three cells, $\mathbf{a}_l$, $\mathbf{b}_l$, and $\mathbf{c}_l$, so the contribution of W^T to each W^U is $W^T/3$, but in the upper layer, it is $W^T/4$ because part of W_T should also be shared by W^U at cell $\mathbf{d}_u$. Here W^U at the bottom of cell $\mathbf{d}_u$ is no longer zero. Therefore, $W^T/4$ of the $W^T/3$ shared by each of the three lower sea grid cells $\mathbf{a}_l$, $\mathbf{b}_l$, and $\mathbf{c}_l$ is purely vertical, and the remaining $W^T/12$ ($= W^T/3 - W^T/4$) flows to cell $\mathbf{d}_u$ through the interface. Gathering these diagonal fluxes from the lower three cells, the total amount entering cell $\mathbf{d}_u$ is certainly $W^T/4$ ($=W^T/12\times 3$). The advected momentum value should be the mean of those at the starting and ending cells of the flux, if the centered difference scheme is used, which is necessary to conserve the total kinetic energy.

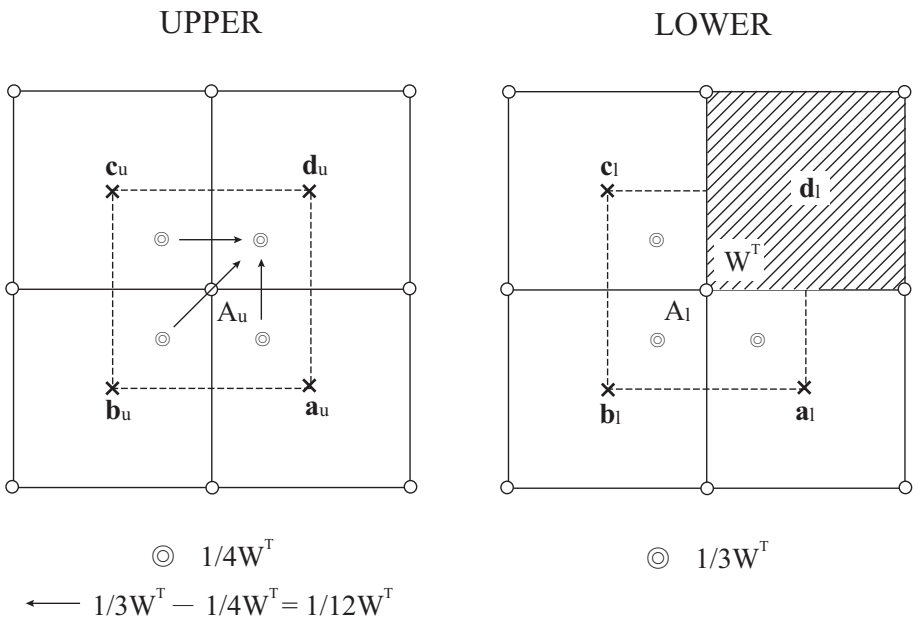

Figure8.2 First example of land-sea patterns, in which all four upper cells are sea cells, with three sea cells and one land cell in the lower layer.

■Example 2 Next, consider an example in which only $\mathbf{b}_l$ is a sea cell in the lower layer, and all four cells are sea cells in the upper layer (Figure 8.3). In the lower layer, W^T is shared only by $\mathbf{b}_l$ but in the upper layer, it is shared by all four cells. Therefore, $W^T/4$ of W^T at cell $\mathbf{b}_l$ is carried vertically upward and the remaining $3W^T/4$ is distributed to the other three cells in the upper layer ($\mathbf{a}_u$, $\mathbf{c}_u$, and $\mathbf{d}_u$), each receiving $W^T/4$.

■Example 3 A third example holds that the upper layer also has land area. In this example, cells $\mathbf{c}_l$, $\mathbf{d}_l$, and $\mathbf{d}_u$ are land cells and the others are sea cells (Figure 8.4). In the lower layer, W^T is shared by two cells ($\mathbf{a}_l$ and $\mathbf{b}_l$) while it is shared by three cells ($\mathbf{a}_u$, $\mathbf{b}_u$, and $\mathbf{c}_u$) in the upper layer. Therefore, from each of $\mathbf{a}_l$ and $\mathbf{b}_l$, $W^T/3$ of $W^T/2$ goes vertically upward and the remaining $W^T/6$ ($= W^T/2 - W^T/3$) goes diagonally upward to cell $\mathbf{c}_u$ with a total amount of $W^T/3$ ($= W^T/6\times 2$).

c. Generalization

The relationship between the land-sea distribution and the vertically and diagonally upward fluxes stated above is generalized for an arbitrary land-sea distribution. Assume cell $\mathbf{d}_l$ is a land but cell $\mathbf{d}_u$ is a sea cell and consider the diagonally upward fluxes coming to cell $\mathbf{d}_u$. We take N_l as the number of sea cells around point A in the lower layer and N_u as the number in the upper layer ($1 \le N_l < N_u \le 4$). Each cell in the lower layer carries W^T/N_l, and W^T/N_u of it goes vertically upward. The remaining

$$W^T/N_l - W^T/N_u = W^T(N_u - N_l)/(N_l N_u) \tag{8.5}$$

should be distributed as diagonally upward fluxes to sea cells in the upper layer at which the lower layer is land. The number of such upper sea cells is $N_u - N_l$ including cell $\mathbf{d}_u$. Thus, each diagonally upward flux coming to cell $\mathbf{d}_u$ is

$$W^T(N_u - N_l)/(N_l N_u) \times 1/(N_u - N_l) = W^T/(N_l N_u). \tag{8.6}$$

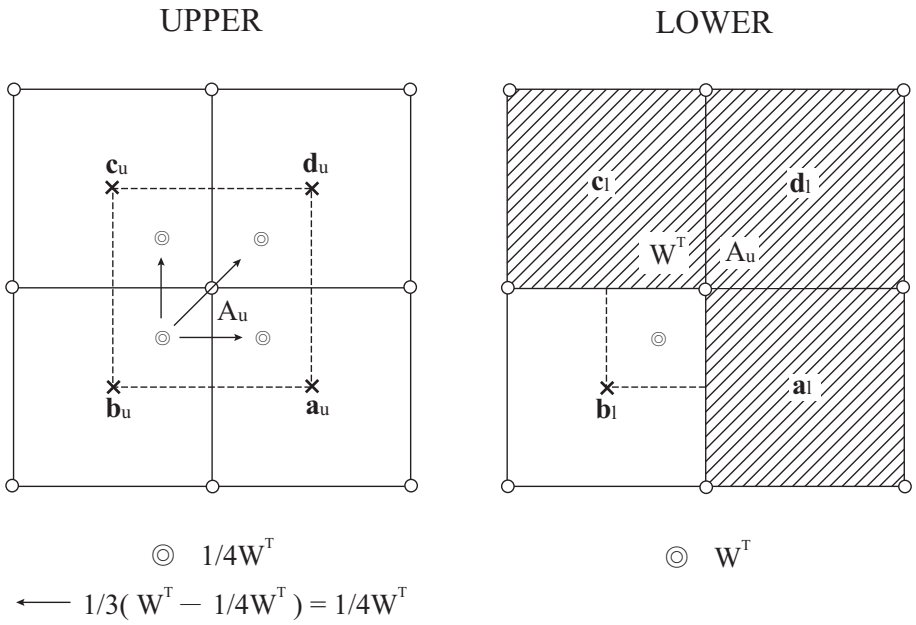

Figure8.3 Second example of land-sea patterns, in which all four upper cells are sea cells, with one sea cell and three land cells in the lower layer.

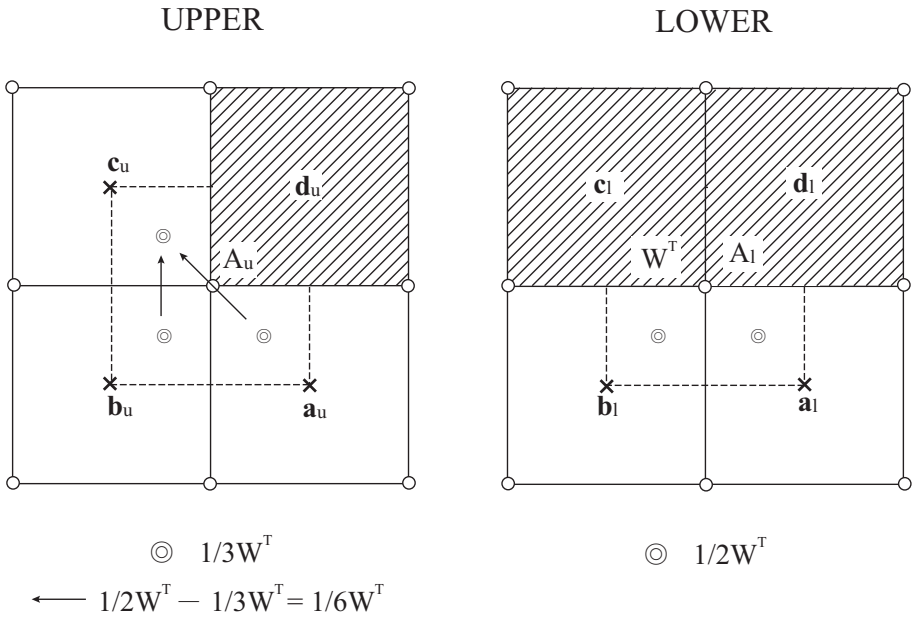

Figure8.4 Third example of land-sea patterns, in which one of the upper cells is a land cell, with two land and two sea cells in the lower layer.

The number of such fluxes coming to the cell $\mathbf{d}_u$ is N_l, so their total is

$$W^T/(N_l N_u) \times N_l = W^T/N_u. \tag{8.7}$$

Based on these discussions we understand the difference between (8.3) and (8.4).

We regard the name of each cell such as $\mathbf{a}_l$ also as a land-sea index. If we assume that $\mathbf{a}_l = 1(0)$ when cell $\mathbf{a}_l$ is a sea (land) cell, then the diagonally upward mass flux and momentum flux coming from cell $\mathbf{a}_l$ to cell $\mathbf{d}_u$ are

$$\mathbf{a}_l W^T/(N_l N_u) \quad \text{and} \quad \mathbf{a}_l W^T (u_{\mathrm{a}_l} + u_{\mathrm{d}_u})/(2N_l N_u), \tag{8.8}$$

where u_{a_l} and u_{d_u} are the velocity at cells $\mathbf{a}_l$ and $\mathbf{d}_u$, respectively. Purely vertical mass flux and momentum flux from cell

$\mathbf{a}_l$ to cell $\mathbf{a}_u$ are expressed as

$$\mathbf{a}_l W^T / N_u \quad \text{and} \quad \mathbf{a}_l W^T (u_{\mathrm{a}_l} + u_{\mathrm{a}_u})/(2N_u), \tag{8.9}$$

respectively, where u_{a_u} is the velocity at cell $\mathbf{a}_u$. Similar formulations apply to cells $\mathbf{b}_l$ and $\mathbf{c}_l$.

Mass and momentum fluxes for W^T at other T-points around cell $\mathbf{d}_u$ should be calculated similarly to complete vertically and diagonally upward momentum advections around cell $\mathbf{d}_u$. When $N_u = N_l$, diagonally upward fluxes need not be considered and only vertical fluxes (8.9) apply.

To summarize, the discrete expression for the vertical flux of zonal momentum that is transported into a U-cell at $(i+\frac{1}{2}, j+\frac{1}{2}, k-\frac{1}{2})$ through its bottom, $F_{\mathbf{L}_{i+\frac{1}{2},j+\frac{1}{2},k}}(u)$, is given as follows:

$$\begin{aligned}
F_{\mathbf{L}_{i+\frac{1}{2},j+\frac{1}{2},k}}(u) =& \frac{1}{2}\left(u_{i+\frac{1}{2},j+\frac{1}{2},k-\frac{1}{2}} + u_{i+\frac{1}{2},j+\frac{1}{2},k+\frac{1}{2}}\right) \times \left[\frac{W^T_{i,j,k}}{N_{i,j,k-\frac{1}{2}}} + \frac{W^T_{i+1,j,k}}{N_{i+1,j,k-\frac{1}{2}}} + \frac{W^T_{i,j+1,k}}{N_{i,j+1,k-\frac{1}{2}}} + \frac{W^T_{i+1,j+1,k}}{N_{i+1,j+1,k-\frac{1}{2}}} \right] \\
&+ \frac{e_{i+\frac{1}{2},j+\frac{1}{2},k-\frac{1}{2}}\left(1 - e_{i+\frac{1}{2},j+\frac{1}{2},k+\frac{1}{2}}\right)}{2} \times \\
&\Big[\Big\{ e_{i-\frac{1}{2},j-\frac{1}{2},k+\frac{1}{2}}\left(u_{i+\frac{1}{2},j+\frac{1}{2},k-\frac{1}{2}} + u_{i-\frac{1}{2},j-\frac{1}{2},k+\frac{1}{2}}\right) + e_{i+\frac{1}{2},j-\frac{1}{2},k+\frac{1}{2}}\left(u_{i+\frac{1}{2},j+\frac{1}{2},k-\frac{1}{2}} + u_{i+\frac{1}{2},j-\frac{1}{2},k+\frac{1}{2}}\right) \\
&+ e_{i-\frac{1}{2},j+\frac{1}{2},k+\frac{1}{2}}\left(u_{i+\frac{1}{2},j+\frac{1}{2},k-\frac{1}{2}} + u_{i-\frac{1}{2},j+\frac{1}{2},k+\frac{1}{2}}\right) \Big\} \times \frac{W^T_{i,j,k}}{N_{i,j,k+\frac{1}{2}} N_{i,j,k-\frac{1}{2}}} \\
&+ \Big\{ e_{i+\frac{1}{2},j-\frac{1}{2},k+\frac{1}{2}}\left(u_{i+\frac{1}{2},j+\frac{1}{2},k-\frac{1}{2}} + u_{i+\frac{1}{2},j-\frac{1}{2},k+\frac{1}{2}}\right) + e_{i+\frac{3}{2},j-\frac{1}{2},k+\frac{1}{2}}\left(u_{i+\frac{1}{2},j+\frac{1}{2},k-\frac{1}{2}} + u_{i+\frac{3}{2},j-\frac{1}{2},k+\frac{1}{2}}\right) \\
&+ e_{i+\frac{3}{2},j+\frac{1}{2},k+\frac{1}{2}}\left(u_{i+\frac{1}{2},j+\frac{1}{2},k-\frac{1}{2}} + u_{i+\frac{3}{2},j+\frac{1}{2},k+\frac{1}{2}}\right) \Big\} \times \frac{W^T_{i+1,j,k}}{N_{i+1,j,k+\frac{1}{2}} N_{i+1,j,k-\frac{1}{2}}} \\
&+ \Big\{ e_{i-\frac{1}{2},j+\frac{1}{2},k+\frac{1}{2}}\left(u_{i+\frac{1}{2},j+\frac{1}{2},k-\frac{1}{2}} + u_{i-\frac{1}{2},j+\frac{1}{2},k+\frac{1}{2}}\right) + e_{i-\frac{1}{2},j+\frac{3}{2},k+\frac{1}{2}}\left(u_{i+\frac{1}{2},j+\frac{1}{2},k-\frac{1}{2}} + u_{i-\frac{1}{2},j+\frac{3}{2},k+\frac{1}{2}}\right) \\
&+ e_{i+\frac{1}{2},j+\frac{3}{2},k+\frac{1}{2}}\left(u_{i+\frac{1}{2},j+\frac{1}{2},k-\frac{1}{2}} + u_{i+\frac{1}{2},j+\frac{3}{2},k+\frac{1}{2}}\right) \Big\} \times \frac{W^T_{i,j+1,k}}{N_{i,j+1,k+\frac{1}{2}} N_{i,j+1,k-\frac{1}{2}}} \\
&+ \Big\{ e_{i+\frac{3}{2},j+\frac{1}{2},k+\frac{1}{2}}\left(u_{i+\frac{1}{2},j+\frac{1}{2},k-\frac{1}{2}} + u_{i+\frac{3}{2},j+\frac{1}{2},k+\frac{1}{2}}\right) + e_{i+\frac{1}{2},j+\frac{3}{2},k+\frac{1}{2}}\left(u_{i+\frac{1}{2},j+\frac{1}{2},k-\frac{1}{2}} + u_{i+\frac{1}{2},j+\frac{3}{2},k+\frac{1}{2}}\right) \\
&+ e_{i+\frac{3}{2},j+\frac{3}{2},k+\frac{1}{2}}\left(u_{i+\frac{1}{2},j+\frac{1}{2},k-\frac{1}{2}} + u_{i+\frac{3}{2},j+\frac{3}{2},k+\frac{1}{2}}\right) \Big\} \times \frac{W^T_{i+1,j+1,k}}{N_{i+1,j+1,k+\frac{1}{2}} N_{i+1,j+1,k-\frac{1}{2}}} \Big],
\end{aligned} \tag{8.10}$$

where $e_{i+\frac{1}{2},j+\frac{1}{2},k-\frac{1}{2}}$ is the land-sea index for a U-cell (unity for sea and zero for land). Note that diagonally upward/downward momentum fluxes may only occur for a U-cell with the sea floor underneath. The momentum fluxes entering and leaving the cells at the lower level ($k = k + \frac{1}{2}$) are individually added or removed from the cell when calculating them.

8.1.2 Horizontal mass flux and its momentum advection

a. Horizontal mass fluxes

We next consider the generalization of the U-cell horizontal mass fluxes for arbitrary coast lines, in order to derive the horizontal momentum advection. To do this, we start with the generalization of the T-cell mass continuity (6.21). Assuming that $e_{i+\frac{1}{2},j+\frac{1}{2}}$ is a land-sea index (unity for sea and zero for land) for U-cell $(i+\frac{1}{2}, j+\frac{1}{2})$, the general formulae for $U^{*T}_{i+\frac{1}{2},j}$ and $V^{*T}_{i,j+\frac{1}{2}}$ are given as

$$\begin{aligned}
U^{*T}_{i+\frac{1}{2},j} =& \frac{1}{2}(e_{i+\frac{1}{2},j-\frac{1}{2}} + e_{i+\frac{1}{2},j+\frac{1}{2}}) u^*_{i+\frac{1}{2},j} \Delta y_{i+\frac{1}{2},j} \Delta z \\
V^{*T}_{i,j+\frac{1}{2}} =& \frac{1}{2}(e_{i-\frac{1}{2},j+\frac{1}{2}} + e_{i+\frac{1}{2},j+\frac{1}{2}}) v^*_{i,j+\frac{1}{2}} \Delta x_{i,j+\frac{1}{2}} \Delta z,
\end{aligned} \tag{8.11}$$

where, $u^*_{i+\frac{1}{2},j}$ and $v^*_{i,j+\frac{1}{2}}$ are the zonal and meridional velocity at the eastern and northern side boundary of a T-cell (i, j) (Eq. 6.26). However, if there are any land cells, only the values at the sea cells are used as in the calculation of Eq. (6.10). Here we neglect the vertical subscript $(k - \frac{1}{2})$.

Substituting these formulae into the T-cell mass continuity (6.21), the X (zonal) component of the mass continuity for

U-cell $(i+\frac{1}{2}, j+\frac{1}{2})$ (6.20), $\mathrm{XMC}^{U}_{i+\frac{1}{2},j+\frac{1}{2}}$, multiplied by its own land-sea signature $e_{i+\frac{1}{2},j+\frac{1}{2}}$, is expressed as

$$
\begin{aligned}
\mathrm{XMC}^{U}_{i+\frac{1}{2},j+\frac{1}{2}} &= e_{i+\frac{1}{2},j+\frac{1}{2}} \frac{\Delta y_{i+\frac{1}{2},j+\frac{1}{2}}}{2} \Delta z \\
&\quad \times \left\{ \frac{1}{N_{i,j}} [(e_{i-\frac{1}{2},j-\frac{1}{2}} + e_{i-\frac{1}{2},j+\frac{1}{2}}) u^{*}_{i-\frac{1}{2},j} - (e_{i+\frac{1}{2},j-\frac{1}{2}} + e_{i+\frac{1}{2},j+\frac{1}{2}}) u^{*}_{i+\frac{1}{2},j}] \right. \\
&\quad + \frac{1}{N_{i+1,j}} [(e_{i+\frac{1}{2},j-\frac{1}{2}} + e_{i+\frac{1}{2},j+\frac{1}{2}}) u^{*}_{i+\frac{1}{2},j} - (e_{i+\frac{3}{2},j-\frac{1}{2}} + e_{i+\frac{3}{2},j+\frac{1}{2}}) u^{*}_{i+\frac{3}{2},j}] \\
&\quad + \frac{1}{N_{i,j+1}} [(e_{i-\frac{1}{2},j+\frac{1}{2}} + e_{i-\frac{1}{2},j+\frac{3}{2}}) u^{*}_{i-\frac{1}{2},j+1} - (e_{i+\frac{1}{2},j+\frac{1}{2}} + e_{i+\frac{1}{2},j+\frac{3}{2}}) u^{*}_{i+\frac{1}{2},j+1}] \\
&\quad \left. + \frac{1}{N_{i+1,j+1}} [(e_{i+\frac{1}{2},j+\frac{1}{2}} + e_{i+\frac{1}{2},j+\frac{3}{2}}) u^{*}_{i+\frac{1}{2},j+1} - (e_{i+\frac{3}{2},j+\frac{1}{2}} + e_{i+\frac{3}{2},j+\frac{3}{2}}) u^{*}_{i+\frac{3}{2},j+1}] \right\} \\
&= e_{i+\frac{1}{2},j+\frac{1}{2}} \frac{\Delta y_{i+\frac{1}{2},j+\frac{1}{2}}}{2} \Delta z \times \left\{ \left[\frac{1}{N_{i,j}} (e_{i-\frac{1}{2},j-\frac{1}{2}} + e_{i-\frac{1}{2},j+\frac{1}{2}}) u^{*}_{i-\frac{1}{2},j} \right. \right. \\
&\quad + \left(-\frac{1}{N_{i,j}} + \frac{1}{N_{i+1,j}} \right) (e_{i+\frac{1}{2},j-\frac{1}{2}} + e_{i+\frac{1}{2},j+\frac{1}{2}}) u^{*}_{i+\frac{1}{2},j} \\
&\quad \left. - \frac{1}{N_{i+1,j}} (e_{i+\frac{3}{2},j-\frac{1}{2}} + e_{i+\frac{3}{2},j+\frac{1}{2}}) u^{*}_{i+\frac{3}{2},j} \right] \\
&\quad + \left[\frac{1}{N_{i,j+1}} (e_{i-\frac{1}{2},j+\frac{1}{2}} + e_{i-\frac{1}{2},j+\frac{3}{2}}) u^{*}_{i-\frac{1}{2},j+1} \right. \\
&\quad + \left(-\frac{1}{N_{i,j+1}} + \frac{1}{N_{i+1,j+1}} \right) (e_{i+\frac{1}{2},j+\frac{1}{2}} + e_{i+\frac{1}{2},j+\frac{3}{2}}) u^{*}_{i+\frac{1}{2},j+1} \\
&\quad \left. \left. - \frac{1}{N_{i+1,j+1}} (e_{i+\frac{3}{2},j+\frac{1}{2}} + e_{i+\frac{3}{2},j+\frac{3}{2}}) u^{*}_{i+\frac{3}{2},j+1} \right] \right\}. \qquad (8.12)
\end{aligned}
$$

Here, recalling

$$
N_{i,j} = e_{i-\frac{1}{2},j-\frac{1}{2}} + e_{i+\frac{1}{2},j-\frac{1}{2}} + e_{i-\frac{1}{2},j+\frac{1}{2}} + e_{i+\frac{1}{2},j+\frac{1}{2}}, \qquad (8.13)
$$

we have,

$$
\begin{aligned}
&\left(-\frac{1}{N_{i,j}} + \frac{1}{N_{i+1,j}} \right) (e_{i+\frac{1}{2},j-\frac{1}{2}} + e_{i+\frac{1}{2},j+\frac{1}{2}}) \\
&\qquad = \frac{1}{N_{i,j}} (e_{i-\frac{1}{2},j-\frac{1}{2}} + e_{i-\frac{1}{2},j+\frac{1}{2}}) - \frac{1}{N_{i+1,j}} (e_{i+\frac{3}{2},j-\frac{1}{2}} + e_{i+\frac{3}{2},j+\frac{1}{2}})
\end{aligned} \qquad (8.14)
$$

and

$$
\begin{aligned}
&\left(-\frac{1}{N_{i,j+1}} + \frac{1}{N_{i+1,j+1}} \right) (e_{i+\frac{1}{2},j+\frac{1}{2}} + e_{i+\frac{1}{2},j+\frac{3}{2}}) \\
&\qquad = \frac{1}{N_{i,j+1}} (e_{i-\frac{1}{2},j+\frac{1}{2}} + e_{i-\frac{1}{2},j+\frac{3}{2}}) - \frac{1}{N_{i+1,j+1}} (e_{i+\frac{3}{2},j+\frac{1}{2}} + e_{i+\frac{3}{2},j+\frac{3}{2}}).
\end{aligned} \qquad (8.15)
$$

Thus, based on (6.24) and (6.25),

$$\begin{aligned}
\mathrm{XMC}^U_{i+\frac{1}{2},j+\frac{1}{2}} &= e_{i+\frac{1}{2},j+\frac{1}{2}} \frac{\Delta y_{i+\frac{1}{2},j+\frac{1}{2}}}{2} \Delta z \Bigg\{ \Bigg[\frac{1}{N_{i,j}} (e_{i-\frac{1}{2},j-\frac{1}{2}} + e_{i-\frac{1}{2},j+\frac{1}{2}})(u^*_{i-\frac{1}{2},j} + u^*_{i+\frac{1}{2},j}) \\
&\quad - \frac{1}{N_{i+1,j}} (e_{i+\frac{3}{2},j-\frac{1}{2}} + e_{i+\frac{3}{2},j+\frac{1}{2}})(u^*_{i+\frac{1}{2},j} + u^*_{i+\frac{3}{2},j}) \Bigg] \\
&\quad + \Bigg[\frac{1}{N_{i,j+1}} (e_{i-\frac{1}{2},j+\frac{1}{2}} + e_{i-\frac{1}{2},j+\frac{3}{2}})(u^*_{i-\frac{1}{2},j+1} + u^*_{i+\frac{1}{2},j+1}) \\
&\quad - \frac{1}{N_{i+1,j+1}} (e_{i+\frac{3}{2},j+\frac{1}{2}} + e_{i+\frac{3}{2},j+\frac{3}{2}})(u^*_{i+\frac{1}{2},j+1} + u^*_{i+\frac{3}{2},j+1}) \Bigg] \Bigg\} \\
&= e_{i+\frac{1}{2},j+\frac{1}{2}} \Bigg[e_{i-\frac{1}{2},j+\frac{1}{2}} \Big(\frac{1}{N_{i,j}} U^U_{i,j} + \frac{1}{N_{i,j+1}} U^U_{i,j+1} \Big) \\
&\quad - e_{i+\frac{3}{2},j+\frac{1}{2}} \Big(\frac{1}{N_{i+1,j}} U^U_{i+1,j} + \frac{1}{N_{i+1,j+1}} U^U_{i+1,j+1} \Big) + e_{i-\frac{1}{2},j-\frac{1}{2}} \frac{1}{N_{i,j}} U^U_{i,j} \\
&\quad - e_{i+\frac{3}{2},j+\frac{3}{2}} \frac{1}{N_{i+1,j+1}} U^U_{i+1,j+1} + e_{i-\frac{1}{2},j+\frac{3}{2}} \frac{1}{N_{i,j+1}} U^U_{i,j+1} - e_{i+\frac{3}{2},j-\frac{1}{2}} \frac{1}{N_{i+1,j}} U^U_{i+1,j} \Bigg].
\end{aligned} \tag{8.16}$$

Adding the Y (meridional) component, YMC (the expression is omitted here), to the above formula, we obtain the horizontal part of the U-cell mass continuity, HMC, as follows:

$$\begin{aligned}
\mathrm{HMC}^U_{i+\frac{1}{2},j+\frac{1}{2}} &= \mathrm{XMC}^U_{i+\frac{1}{2},j+\frac{1}{2}} + \mathrm{YMC}^U_{i+\frac{1}{2},j+\frac{1}{2}} \\
&= e_{i+\frac{1}{2},j+\frac{1}{2}} \\
&\quad \times \Bigg[e_{i-\frac{1}{2},j+\frac{1}{2}} \Big(\frac{1}{N_{i,j}} U^U_{i,j} + \frac{1}{N_{i,j+1}} U^U_{i,j+1} \Big) - e_{i+\frac{3}{2},j+\frac{1}{2}} \Big(\frac{1}{N_{i+1,j}} U^U_{i+1,j} + \frac{1}{N_{i+1,j+1}} U^U_{i+1,j+1} \Big) \\
&\quad + e_{i+\frac{1}{2},j-\frac{1}{2}} \Big(\frac{1}{N_{i,j}} V^U_{i,j} + \frac{1}{N_{i+1,j}} V^U_{i+1,j} \Big) - e_{i+\frac{1}{2},j+\frac{3}{2}} \Big(\frac{1}{N_{i,j+1}} V^U_{i,j+1} + \frac{1}{N_{i+1,j+1}} V^U_{i+1,j+1} \Big) \\
&\quad + e_{i-\frac{1}{2},j-\frac{1}{2}} \frac{1}{N_{i,j}} (U^U_{i,j} + V^U_{i,j}) - e_{i+\frac{3}{2},j+\frac{3}{2}} \frac{1}{N_{i+1,j+1}} (U^U_{i+1,j+1} + V^U_{i+1,j+1}) \\
&\quad + e_{i-\frac{1}{2},j+\frac{3}{2}} \frac{1}{N_{i,j+1}} (U^U_{i,j+1} - V^U_{i,j+1}) - e_{i+\frac{3}{2},j-\frac{1}{2}} \frac{1}{N_{i+1,j}} (U^U_{i+1,j} - V^U_{i+1,j}) \Bigg].
\end{aligned} \tag{8.17}$$

Assuming mass fluxes $M_{\mathbf{E}}, M_{\mathbf{N}}, M_{\mathbf{NE}}, M_{\mathbf{SE}}$ as follows:

$$\begin{aligned}
M_{\mathbf{E}_{i,j+\frac{1}{2}}} &= e_{i+\frac{1}{2},j+\frac{1}{2}} e_{i-\frac{1}{2},j+\frac{1}{2}} \Big(\frac{1}{N_{i,j}} U^U_{i,j} + \frac{1}{N_{i,j+1}} U^U_{i,j+1} \Big), \\
M_{\mathbf{N}_{i+\frac{1}{2},j}} &= e_{i+\frac{1}{2},j+\frac{1}{2}} e_{i+\frac{1}{2},j-\frac{1}{2}} \Big(\frac{1}{N_{i,j}} V^U_{i,j} + \frac{1}{N_{i+1,j}} V^U_{i+1,j} \Big), \\
M_{\mathbf{NE}_{i,j}} &= e_{i+\frac{1}{2},j+\frac{1}{2}} e_{i-\frac{1}{2},j-\frac{1}{2}} \frac{1}{N_{i,j}} (U^U_{i,j} + V^U_{i,j}), \\
M_{\mathbf{SE}_{i,j}} &= e_{i-\frac{1}{2},j+\frac{1}{2}} e_{i+\frac{1}{2},j-\frac{1}{2}} \frac{1}{N_{i,j}} (U^U_{i,j} - V^U_{i,j}),
\end{aligned} \tag{8.18}$$

then,

$$\begin{aligned}
\mathrm{HMC}^U_{i+\frac{1}{2},j+\frac{1}{2}} =& M_{\mathbf{E}_{i,j+\frac{1}{2}}} - M_{\mathbf{E}_{i+1,j+\frac{1}{2}}} + M_{\mathbf{N}_{i+\frac{1}{2},j}} - M_{\mathbf{N}_{i+\frac{1}{2},j+1}} \\
&+ M_{\mathbf{NE}_{i,j}} - M_{\mathbf{NE}_{i+1,j+1}} + M_{\mathbf{SE}_{i,j+1}} - M_{\mathbf{SE}_{i+1,j}}.
\end{aligned} \tag{8.19}$$

Here, $M_{\mathbf{E}}$ and $M_{\mathbf{N}}$ are axis-parallel mass fluxes, and $M_{\mathbf{NE}}$ and $M_{\mathbf{SE}}$ are horizontally diagonal ones (Figure 8.5).

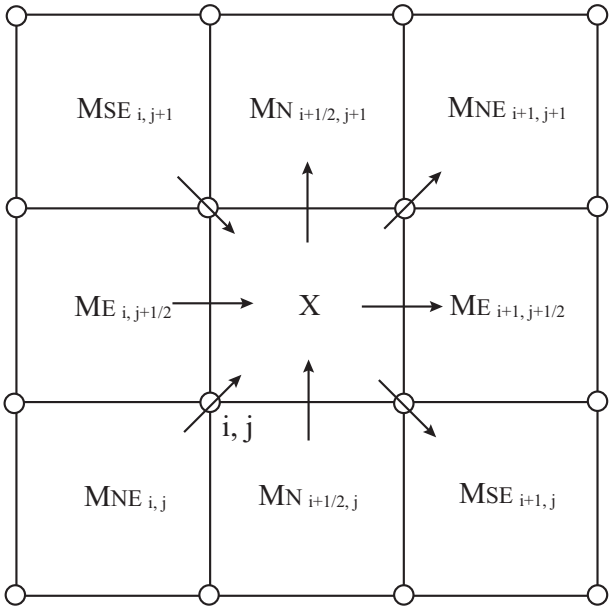

Figure8.5 Distribution of generalized mass fluxes for U-cell $(i + 1/2, j + 1/2)$

If we derive the formula for the standard case from (8.17) (all of N are 4),

$$\begin{aligned}\mathrm{HMC}^U_{i+\frac{1}{2},j+\frac{1}{2}} = \frac{1}{2}\Big[&\frac{1}{2}(U^U_{i,j}+U^U_{i,j+1})-\frac{1}{2}(U^U_{i+1,j}+U^U_{i+1,j+1})\\ &+\frac{1}{2}(V^U_{i,j}+V^U_{i,j+1})-\frac{1}{2}(V^U_{i+1,j}+V^U_{i+1,j+1})\Big]\\ +\frac{1}{2}\Big[&\frac{1}{2}(U^U_{i,j}+V^U_{i,j})-\frac{1}{2}(U^U_{i+1,j+1}+V^U_{i+1,j+1})\\ &+\frac{1}{2}(U^U_{i,j+1}-V^U_{i,j+1})-\frac{1}{2}(U^U_{i+1,j}-V^U_{i+1,j})\Big].\end{aligned} \tag{8.20}$$

This expression means that the horizontal mass flux convergence is a mean of those of the axis-parallel mass fluxes (6.23) and of the diagonal ones (6.29). However, their weighting factors α and β are both $1/2$ in the present case, while $(\alpha, \beta) = (2/3, 1/3)$ for the generalized Arakawa scheme, which conserves quasi-enstrophy such as $(\delta v/\delta x)^2$ and $(\delta u/\delta y)^2$ in a horizontally non-divergent flow.

b. Horizontal momentum advection

For the standard case away from land, we have the freedom to choose weights $(\alpha : \beta)$ for averaging the convergences of the axis-parallel and the horizontally diagonal mass fluxes, as long as $\alpha + \beta = 1$, as seen in (8.20). In MRI.COM $\alpha = 2/3$ and $\beta = 1/3$ are chosen for the standard case so that the momentum advection terms lead to the generalized Arakawa scheme. In this case the zonal momentum advection term is expressed by convergence of the horizontal momentum fluxes

Table8.1 Definition of a land-sea index, the index identifying each case (column **A**), the coefficient of $U^U_{i,j}$ in the axis-parallel mass flux (column **B**), and the coefficient of $U^U_{i,j}$ in the horizontally diagonal mass flux (column **C**), for eight combinations of indices **a**, **b**, and **c** in Figure 8.2b (see the main text). Cell **d** is assumed to be a sea cell, and the momentum advection by means of $U^U_{i,j}$ into and from cell **d** is generalized. Note that $U^U_{i,j}$ is identically zero for cases 5 and 8 (**b** = **c** = 0).

CASE n	Land-sea index **a**	**b**	**c**	**A**	**B** Coefficient of $U^U_{i,j}$ (axis-parallel) +	**C** Coefficient of $U^U_{i,j}$ (horizontally-diagonal) ×
1	1	1	1	**abc**	1/3	1/6
2	1	1	0	**ab**(1 − **c**)	0	1/3
3	1	0	1	**ab**(1 − **b**)**c**	1/3	0
4	0	1	1	(1 − **a**)**bc**	1/3	1/3
5	1	0	0	–	0	0
6	0	1	0	(1 − **a**)**b**(1 − **c**)	0	1/2
7	0	0	1	(1 − **a**)(1 − **b**)**c**	1/2	0
8	0	0	0	–	0	0

as follows:

$$
\begin{aligned}
\mathrm{CAD}_{i+\frac{1}{2},j+\frac{1}{2}}(u) = \frac{2}{3}\Big[&\frac{1}{2}(u_{i-\frac{1}{2},j+\frac{1}{2}}+u_{i+\frac{1}{2},j+\frac{1}{2}})\frac{1}{2}(U^U_{i,j}+U^U_{i,j+1})\\
&-\frac{1}{2}(u_{i+\frac{1}{2},j+\frac{1}{2}}+u_{i+\frac{3}{2},j+\frac{1}{2}})\frac{1}{2}(U^U_{i+1,j}+U^U_{i+1,j+1})\\
&+\frac{1}{2}(u_{i+\frac{1}{2},j-\frac{1}{2}}+u_{i+\frac{1}{2},j+\frac{1}{2}})\frac{1}{2}(V^U_{i,j}+V^U_{i+1,j})\\
&-\frac{1}{2}(u_{i+\frac{1}{2},j+\frac{1}{2}}+u_{i+\frac{1}{2},j+\frac{3}{2}})\frac{1}{2}(V^U_{i,j+1}+V^U_{i+1,j+1})\Big]\\
+\frac{1}{3}\Big[&\frac{1}{2}(u_{i+\frac{1}{2},j+\frac{1}{2}}+u_{i-\frac{1}{2},j-\frac{1}{2}})\frac{1}{2}(U^U_{i,j}+V^U_{i,j})\\
&-\frac{1}{2}(u_{i+\frac{1}{2},j+\frac{1}{2}}+u_{i+\frac{3}{2},j+\frac{3}{2}})\frac{1}{2}(U^U_{i+1,j+1}+V^U_{i+1,j+1})\\
&+\frac{1}{2}(u_{i+\frac{1}{2},j+\frac{1}{2}}+u_{i-\frac{1}{2},j+\frac{3}{2}})\frac{1}{2}(U^U_{i,j+1}-V^U_{i,j+1})\\
&-\frac{1}{2}(u_{i+\frac{1}{2},j+\frac{1}{2}}+u_{i+\frac{3}{2},j-\frac{1}{2}})\frac{1}{2}(U^U_{i+1,j}-V^U_{i+1,j})\Big]
\end{aligned}
\tag{8.21}
$$

This scheme under Arakawa's B-grid arrangement conserves the quasi-enstrophies ($(\partial u/\partial y)^2$ and $(\partial v/\partial x)^2$) in a horizontally non-divergent flow.

To merge the generalized Arakawa scheme for the standard case into the general form of the horizontal mass flux expressed in Figure 8.5 and related momentum flux, let us examine the axis-parallel and horizontally diagonal mass flux associated with $U^U_{i,j}$, taking topography into account. Look at Figure 8.2b, where letters **a**, **b**, **c**, and **d** designate the land-sea index and names of U-cells. Cell **d** is assumed to be a sea cell (**d** = 1). We analyze two kinds of mass fluxes associated with $U^U_{i,j}$ under different combinations of **a**, **b**, and **c** (eight cases), as indicated in the first column in Table 8.1. Column (A) corresponds to an index, which is unity for its own combination and zero for all other combinations. Column (B) lists the coefficient of $U^U_{i,j}$ in the axis-parallel mass flux of the U-cell mass continuity (8.17). Column (C) indicates the coefficient of $U^U_{i,j}$ in the horizontally diagonal mass flux of (8.17).

The generalized coefficient of $U^U_{i,j}$ in the axis-parallel mass flux (c_1) is obtained by summing the product of **A** and **B** over the eight cases. Similarly, the generalized coefficient in the horizontally diagonal mass flux (c_2) is obtained by the

summing the product of **A** and **C**. That is,

$$c_1 = \sum_{n=1}^{8} \mathbf{A}_n \mathbf{B}_n = \frac{1}{6}\mathbf{c}(\mathbf{ab} - \mathbf{a} - \mathbf{b}+3)$$

and

$$c_2 = \sum_{n=1}^{8} \mathbf{A}_n \mathbf{C}_n = \frac{1}{6}\mathbf{b}(3-\mathbf{a} - \mathbf{c}). \tag{8.22}$$

Then, the axis-parallel and the horizontally diagonal flux of zonal momentum (u) related with $U^U_{i,j}$, multiplied by the land-sea index **d**, are

$$\frac{\mathbf{d}}{2}(u_{\mathbf{c}} + u_{\mathbf{d}})c_1 U^U_{i,j} = \frac{1}{2}(u_{\mathbf{c}} + u_{\mathbf{d}})\frac{1}{6}\mathbf{cd}(\mathbf{ab} - \mathbf{a} - \mathbf{b}+3)U^U_{i,j},$$

and

$$\frac{\mathbf{d}}{2}(u_{\mathbf{b}} + u_{\mathbf{d}})c_2 U^U_{i,j} = \frac{1}{2}(u_{\mathbf{b}} + u_{\mathbf{d}})\frac{1}{6}\mathbf{bd}(3-\mathbf{a} - \mathbf{c})U^U_{i,j}, \tag{8.23}$$

respectively.

The resultant momentum fluxes are as follows:

$$\begin{aligned}
F_{\mathbf{E}_{i,j+\frac{1}{2}}}(u) &= \frac{1}{2}(u_{i-\frac{1}{2},j+\frac{1}{2}} + u_{i+\frac{1}{2},j+\frac{1}{2}})M_{\mathbf{E}_{i,j+\frac{1}{2}}},\\
F_{\mathbf{N}_{i+\frac{1}{2},j}}(u) &= \frac{1}{2}(u_{i+\frac{1}{2},j-\frac{1}{2}} + u_{i+\frac{1}{2},j+\frac{1}{2}})M_{\mathbf{N}_{i+\frac{1}{2},j}},\\
F_{\mathbf{NE}_{i,j}}(u) &= \frac{1}{2}(u_{i+\frac{1}{2},j+\frac{1}{2}} + u_{i-\frac{1}{2},j-\frac{1}{2}})M_{\mathbf{NE}_{i,j}},\\
F_{\mathbf{SE}_{i,j}}(u) &= \frac{1}{2}(u_{i-\frac{1}{2},j+\frac{1}{2}} + u_{i+\frac{1}{2},j-\frac{1}{2}})M_{\mathbf{SE}_{i,j}},
\end{aligned} \tag{8.24}$$

where

$$\begin{aligned}
M_{\mathbf{E}_{i,j+\frac{1}{2}}} &= \frac{1}{6}(C_{\mathbf{XN}_{i,j}}U^U_{i,j} + C_{\mathbf{XS}_{i,j+1}}U^U_{i,j+1}),\\
M_{\mathbf{N}_{i+\frac{1}{2},j}} &= \frac{1}{6}(C_{\mathbf{YE}_{i,j}}V^U_{i,j} + C_{\mathbf{YW}_{i+1,j}}V^U_{i+1,j}),\\
M_{\mathbf{NE}_{i,j}} &= \frac{1}{6}C_{\mathbf{NE}_{i,j}}(U^U_{i,j} + V^U_{i,j}),\\
M_{\mathbf{SE}_{i,j}} &= \frac{1}{6}C_{\mathbf{SE}_{i,j}}(U^U_{i,j} - V^U_{i,j}),
\end{aligned} \tag{8.25}$$

and

$$\begin{aligned}
C_{\mathbf{XN}_{i,j}} &= e_{i+\frac{1}{2},j+\frac{1}{2}}e_{i-\frac{1}{2},j+\frac{1}{2}}(e_{i+\frac{1}{2},j-\frac{1}{2}}e_{i-\frac{1}{2},j-\frac{1}{2}} - e_{i+\frac{1}{2},j-\frac{1}{2}} - e_{i-\frac{1}{2},j-\frac{1}{2}} + 3),\\
C_{\mathbf{XS}_{i,j}} &= e_{i+\frac{1}{2},j-\frac{1}{2}}e_{i-\frac{1}{2},j-\frac{1}{2}}(e_{i+\frac{1}{2},j+\frac{1}{2}}e_{i-\frac{1}{2},j+\frac{1}{2}} - e_{i+\frac{1}{2},j+\frac{1}{2}} - e_{i-\frac{1}{2},j+\frac{1}{2}} + 3),\\
C_{\mathbf{YE}_{i,j}} &= e_{i+\frac{1}{2},j+\frac{1}{2}}e_{i+\frac{1}{2},j-\frac{1}{2}}(e_{i-\frac{1}{2},j+\frac{1}{2}}e_{i-\frac{1}{2},j-\frac{1}{2}} - e_{i-\frac{1}{2},j+\frac{1}{2}} - e_{i-\frac{1}{2},j-\frac{1}{2}} + 3),\\
C_{\mathbf{YW}_{i,j}} &= e_{i-\frac{1}{2},j+\frac{1}{2}}e_{i-\frac{1}{2},j-\frac{1}{2}}(e_{i+\frac{1}{2},j+\frac{1}{2}}e_{i+\frac{1}{2},j-\frac{1}{2}} - e_{i+\frac{1}{2},j+\frac{1}{2}} - e_{i+\frac{1}{2},j-\frac{1}{2}} + 3),\\
C_{\mathbf{NE}_{i,j}} &= e_{i+\frac{1}{2},j+\frac{1}{2}}e_{i-\frac{1}{2},j-\frac{1}{2}}(3 - e_{i-\frac{1}{2},j+\frac{1}{2}} - e_{i+\frac{1}{2},j-\frac{1}{2}}),\\
C_{\mathbf{SE}_{i,j}} &= e_{i-\frac{1}{2},j+\frac{1}{2}}e_{i+\frac{1}{2},j-\frac{1}{2}}(3 - e_{i+\frac{1}{2},j+\frac{1}{2}} - e_{i-\frac{1}{2},j-\frac{1}{2}}).
\end{aligned} \tag{8.26}$$

Finally, convergence of the horizontal momentum fluxes is written as

$$\begin{aligned}
\mathrm{CAD}_{i+\frac{1}{2},j+\frac{1}{2}}(u) =& F_{\mathbf{E}_{i,j+\frac{1}{2}}}(u) - F_{\mathbf{E}_{i+1,j+\frac{1}{2}}}(u) + F_{\mathbf{N}_{i+\frac{1}{2},j}}(u) - F_{\mathbf{N}_{i+\frac{1}{2},j+1}}(u)\\
&+ F_{\mathbf{NE}_{i,j}}(u) - F_{\mathbf{NE}_{i+1,j+1}}(u) + F_{\mathbf{SE}_{i,j+1}}(u) - F_{\mathbf{SE}_{i+1,j}}(u).
\end{aligned} \tag{8.27}$$

This is the discrete expression for the advection term of the zonal momentum $\frac{1}{h_\mu h_\psi}\left\{\frac{\partial(z_s h_\psi uu)}{\partial\mu} + \frac{\partial(z_s h_\mu vu)}{\partial\psi}\right\}$ under the finite volume method (equations being integrated over a U-cell).

8.2 Pressure gradient term

In the split-explicit solution method, the pressure gradient term of the horizontal momentum equation is separated into barotropic (fast) and baroclinic (slow) terms (Eq. 2.56). Its form is

$$\underbrace{\frac{1}{\rho_0}\nabla_s(p_a+g\rho_0\eta)}_{\text{fast}}+\underbrace{\overbrace{\frac{1}{\rho_0}\nabla_s\left[g\int_{z(s)}^{\eta}\rho' dz\right]}^{\text{pressure perturbation}}+\overbrace{\frac{g\rho'}{\rho_0}\nabla_s z}^{\text{geopotential}}}_{\text{slow}}. \tag{8.28}$$

Here, we use symbol s to indicate z^* for brevity, and so ∇_s means ∇_{z^*}. These three terms correspond to the first, second, and third terms in the r.h.s. of (8.1) and (8.2). From the perspective of the momentum conservation, the finite difference of the pressure gradient terms should be expressed so that the pressure at the interface of adjacent cells is common, giving only boundary pressures after horizontal integration. This is not difficult for the barotropic mode. The baroclinic mode should be considered carefully. Among the baroclinic terms in (8.28), the former is called the pressure perturbation term and the latter is called the geopotential term.

Because sea-floor depth is defined at U-cells in MRI.COM, it is not necessary to consider the horizontal gradient of the sea floor in calculating the pressure gradient for a bottom U-cell unlike σ-coordinate models and possibly the depth-coordinate models that employ staggered grid arrangements different from MRI.COM. This makes the finite difference expression simple, and the pressure gradient error may be expected to be small. However, this simplicity does not hold for the bottom boundary layer (BBL). The treatment of the pressure gradient term for BBL is explained in Chapter 16.

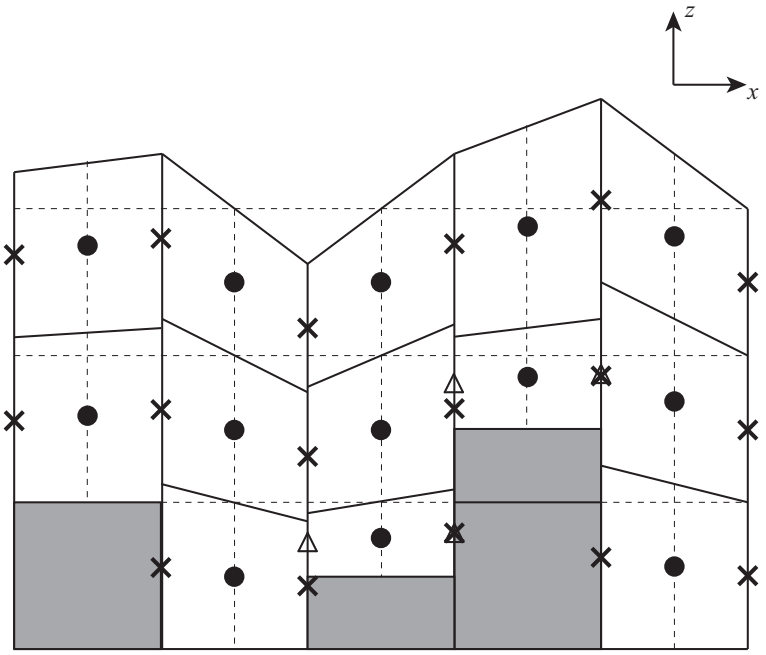

Figure8.6 Illustration of a vertical slice through a set of grid cells in the x-z plane for z^* coordinate. The center point in each cell (•) is a velocity point, and the pressure gradient term is calculated at this point. The cross (×) is a tracer point, and pressure is calculated here. The triangle (△), whose z^* value is that of the adjacent U-point of the bottom U-cell, is the hydrostatic pressure point which is used to evaluate pressure gradient for the bottom U-cell.

a. Discretization of the pressure perturbation term

Figure 8.6 shows the grid points on the x-z plane relevant to calculating pressure gradient terms. Pressures are defined on T-points. Because the actual vertical integration distances are different between adjacent T-points for z^* coordinate, it is appropriate to differentiate pressures after computing them at T-points rather than vertically integrating the pressure gradient as in z coordinate. However, the round-off error due to the differentiation of vertically integrated quantity would

increase with depth. To avoid this, we add contribution from the integration over one vertical grid to the pressure gradient term at the upper vertical level, as explained below.

Introducing pressure perturbation p', the pressure perturbation term in Eq. (8.28) is expressed as

$$\frac{1}{\rho_0}\nabla_s\left[g\int_{z(s)}^{\eta}\rho' dz\right] = \frac{1}{\rho_0}\nabla_s p', \tag{8.29}$$

$$\text{where} \quad p' = g\int_{z(s)}^{\eta}\rho' dz. \tag{8.30}$$

A simple discrete expression would be given as follows ($1/\rho_0$ is omitted):

$$(\nabla_s p')_{i+\frac{1}{2},j+\frac{1}{2},k-\frac{1}{2}} = \hat{\mathbf{x}}\frac{\frac{p'_{i+1,j+1,k-\frac{1}{2}}+p'_{i+1,j,k-\frac{1}{2}}}{2} - \frac{p'_{i,j+1,k-\frac{1}{2}}+p'_{i,j,k-\frac{1}{2}}}{2}}{\Delta x_{i+\frac{1}{2},j+\frac{1}{2}}} + \hat{\mathbf{y}}\frac{\frac{p'_{i+1,j+1,k-\frac{1}{2}}+p'_{i,j+1,k-\frac{1}{2}}}{2} - \frac{p'_{i+1,j,k-\frac{1}{2}}+p'_{i,j,k-\frac{1}{2}}}{2}}{\Delta y_{i+\frac{1}{2},j+\frac{1}{2}}}, \tag{8.31}$$

$$\text{where} \quad p'_{i,j,k-\frac{1}{2}} = g\sum_{l=1}^{k-1}(\rho')_{i,j,l-\frac{1}{2}}(\mathtt{dzt})_{i,j,l-\frac{1}{2}} + g(\rho')_{i,j,k-\frac{1}{2}}\frac{(\mathtt{dzt})_{i,j,k-\frac{1}{2}}}{2}. \tag{8.32}$$

However, because density perturbation (ρ') would generally take similar values in adjacent grids, the pressure perturbation (p') would also take similar values in adjacent grids. The round-off error caused by differentiation would increase with the depth. To avoid this round-off error, we use another discrete expression given as follows:

$$\begin{aligned}(\nabla_s p')_{i+\frac{1}{2},j+\frac{1}{2},k-\frac{1}{2}} &= (\nabla_s p')_{i+\frac{1}{2},j+\frac{1}{2},k-\frac{3}{2}} + \left\{(\nabla_s p')_{i+\frac{1}{2},j+\frac{1}{2},k-\frac{1}{2}} - (\nabla_s p')_{i+\frac{1}{2},j+\frac{1}{2},k-\frac{3}{2}}\right\} \\ &= (\nabla_s p')_{i+\frac{1}{2},j+\frac{1}{2},k-\frac{3}{2}} + \hat{\mathbf{x}}\frac{\frac{\Delta p'_{i+1,j+1,k-1}+\Delta p'_{i+1,j,k-1}}{2} - \frac{\Delta p'_{i,j+1,k-1}+\Delta p'_{i,j,k-1}}{2}}{\Delta x_{i+\frac{1}{2},j+\frac{1}{2}}} \\ &\quad + \hat{\mathbf{y}}\frac{\frac{\Delta p'_{i+1,j+1,k-1}+\Delta p'_{i,j+1,k-1}}{2} - \frac{\Delta p'_{i+1,j,k-1}+\Delta p'_{i,j,k-1}}{2}}{\Delta y_{i+\frac{1}{2},j+\frac{1}{2}}},\end{aligned} \tag{8.33}$$

where

$$\Delta p'_{i,j,k-1} \equiv p'_{i,j,k-\frac{1}{2}} - p'_{i,j,k-\frac{3}{2}} = g(\rho')_{i,j,k-\frac{3}{2}}\frac{(\mathtt{dzt})_{i,j,k-\frac{1}{2}}}{2} + g(\rho')_{i,j,k-\frac{1}{2}}\frac{(\mathtt{dzt})_{i,j,k-\frac{1}{2}}}{2}. \tag{8.34}$$

b. Discretization of the geopotential term

The geopotential term is also discretized so that a round-off error is minimized. Considering that the time-dependent part of the actual depth $z = z(s)$ is due to the perturbation ($z'(s)$) from the state of rest ($z_0(s)$) caused by the sea level variation, taking differentiation for $z(s)$ at depth is not quite accurate owing to the numerical round-off. Then we separate the actual depth as $z(s) = z_0(s) + z'(s)$ and only use $z'(s)$ for horizontal gradient of geopotential, that is,

$$\frac{g\rho'}{\rho_0}\nabla_s z = \frac{g\rho'}{\rho_0}\nabla_s z'(s). \tag{8.35}$$

Here, we used the fact that the depth of the constant s-surface is flat at the state of rest, i.e. $\nabla_s z_0(s) = 0$. (Again, we cannot use this simplicity for the bottom boundary layer. See Chapter 16 for details.) Then, the term is differentiated as

$$\begin{aligned}&\left[\frac{g\rho'}{\rho_0}\nabla_s z'\right]_{i+\frac{1}{2},j+\frac{1}{2}} \\ &= \frac{g}{\rho_0}\left\{\left[\frac{\frac{\rho'_{i+1,j}+\rho'_{i,j}}{2}\frac{z'_{i+1,j}-z'_{i,j}}{\Delta x_{i+\frac{1}{2},j}} + \frac{\rho'_{i+1,j+1}+\rho'_{i,j+1}}{2}\frac{z'_{i+1,j+1}-z'_{i,j+1}}{\Delta x_{i+\frac{1}{2},j+1}}}{2}\hat{\mathbf{x}}\right] + \left[\frac{\frac{\rho'_{i,j+1}+\rho'_{i,j}}{2}\frac{z'_{i,j+1}-z'_{i,j}}{\Delta y_{i,j+\frac{1}{2}}} + \frac{\rho'_{i+1,j+1}+\rho'_{i+1,j}}{2}\frac{z'_{i+1,j+1}-z'_{i+1,j}}{\Delta y_{i+1,j+\frac{1}{2}}}}{2}\hat{\mathbf{y}}\right]\right\}.\end{aligned} \tag{8.36}$$

Here, we follow the expression presented in Section 3.3.1 of the reference manual of GFDL-MOM.

c. The sea-floor grid (except for bottom boundary layer)

Owing to the introduction of the partial cell, the grid width of the bottom U-cell may depend on the horizontal position. The pressure gradient term in (8.28) is the gradient of pressure on constant $s(z^*)$-surface. Thus, the pressure gradient force on a partial U-cell is evaluated using the pressure perturbation p' obtained by integrating to the depth where velocity is defined on z^* coordinate (the central depth of the bottom U-cell). These are the points with triangle ($\triangle$) symbols in Figure 3.6.

To calculate the pressure gradient, the actual depth of the vertical level where velocity is defined for the bottom U-cell ($s = s^U_{k=kbtm}$) must be obtained at all four corner T-points of a U-cell. Here, these are determined using the ratio of the half width of a U-cell $\frac{1}{2}\Delta s^U$ to the width of a T-cell Δs^T:

$$z^U_{kbtm} = z^T_{kbtm-1} - \Delta z^T_{kbtm} \frac{\Delta s^U_{kbtm}}{2\Delta s^T_{kbtm}}. \tag{8.37}$$

The depth anomaly used for computing geopotential gradient anomaly may be obtained in the same way:

$$z'^U_{kbtm} = z'^T_{kbtm-1} - \Delta z'^T_{kbtm} \frac{\Delta s^U_{kbtm}}{2\Delta s^T_{kbtm}}. \tag{8.38}$$

The finite difference expression for horizontal gradient is formally the same as (8.33) and (8.36). However, the vertical integration to obtain p' is performed to the depth where velocity is defined for the bottom U-cell. Geopotential term is evaluated using a depth anomaly of $s(z^*)$-surface. Thus, on the same vertical level, the algorism is different depending on whether it is bottom cell or not.

8.3 Viscosity

The viscosity in an ocean general circulation model seeks to attenuate numerical noise rather than parameterizing the subgrid-scale momentum transport. The momentum advection scheme should conserve the total kinetic energy in the general three-dimensional flows and the total enstrophy in the two-dimensional flows. Therefore, spatially and temporally centered discretization should be used, although this inevitably produces near-grid-size noise accompanying numerical dispersion. In eddy-resolving models, the current velocity and the numerical noise are greater than those of eddy-less models. A biharmonic viscosity scheme has been widely used to reduce numerical noise while maintaining the eddy structure.

The viscosity term is represented by $\mathcal{V}$ and is calculated separately in the lateral and vertical directions, i.e., the fourth and fifth terms, respectively, on the r.h.s. of (8.1) and (8.2). For horizontal viscosity, the harmonic (default) or biharmonic (`VISBIHARM` option) scheme can be selected. Anisotropy of viscosity with respect to the flow direction can be applied (`VISANISO` option) when harmonic viscosity is chosen. The viscosity coefficient is a constant by default but can be determined as a function of local velocity gradients and grid-size (`SMAGOR` option).

For vertical viscosity, the harmonic scheme is used and the local coefficient is the larger one of the background constant and the value calculated from a turbulence closure scheme. A parameterization of bottom friction (Weatherly et al., 1980) is adopted at the lowest layer.

8.3.1 Horizontal viscosity

The specific form for harmonic viscosity is shown here. Horizontal tension D_T and shear D_S are defined as follows:

$$D_T = h_\psi \frac{\partial}{h_\mu \partial\mu}\left(\frac{u}{h_\psi}\right) - h_\mu \frac{\partial}{h_\psi \partial\psi}\left(\frac{v}{h_\mu}\right), \tag{8.39}$$

$$D_S = h_\psi \frac{\partial}{h_\mu \partial\mu}\left(\frac{v}{h_\psi}\right) + h_\mu \frac{\partial}{h_\psi \partial\psi}\left(\frac{u}{h_\mu}\right). \tag{8.40}$$

The viscosity terms are

$$\mathcal{V}_u = \frac{1}{h^2_\psi}\frac{\partial}{h_\mu \partial\mu}\left(h^2_\psi \sigma_T\right) + \frac{1}{h^2_\mu}\frac{\partial}{h_\psi \partial\psi}\left(h^2_\mu \sigma_S\right), \tag{8.41}$$

$$\mathcal{V}_v = \frac{1}{h^2_\psi}\frac{\partial}{h_\mu \partial\mu}\left(h^2_\psi \sigma_S\right) - \frac{1}{h^2_\mu}\frac{\partial}{h_\psi \partial\psi}\left(h^2_\mu \sigma_T\right), \tag{8.42}$$

where $\sigma_T = \nu_H D_T$ and $\sigma_S = \nu_H D_S$, and ν_H is the horizontal viscosity coefficient. The above representation of the viscous term was derived by Bryan (1969) and is consistent with Smagorinsky (1963).

If we take $h_\mu = 1, h_\psi = 1$, the coordinate system is Cartesian. In this case, the viscosity term is reduced to the Laplacian form if the viscosity coefficient is a constant. In the geographic coordinate system, where $(\mu, \psi) = (\lambda, \phi)$, $h_\lambda = a\cos\phi$, and $h_\phi = a$, tension and shear are

$$D_T = \frac{1}{a\cos\phi}\frac{\partial u}{\partial \lambda} - \frac{1}{a}\frac{\partial v}{\partial \phi} - \frac{v}{a}\tan\phi, \tag{8.43}$$

$$D_S = \frac{1}{a\cos\phi}\frac{\partial v}{\partial \lambda} + \frac{1}{a}\frac{\partial u}{\partial \phi} + \frac{u}{a}\tan\phi. \tag{8.44}$$

The viscosity terms in this case are

$$\mathcal{V}_u = \frac{1}{a\cos\phi}\frac{\partial}{\partial \lambda}\sigma_T + \frac{1}{a}\frac{\partial}{\partial \phi}\sigma_S - \sigma_S\frac{2\tan\phi}{a}, \tag{8.45}$$

$$\mathcal{V}_v = \frac{1}{a\cos\phi}\frac{\partial}{\partial \lambda}\sigma_S - \frac{1}{a}\frac{\partial}{\partial \phi}\sigma_T + \sigma_T\frac{2\tan\phi}{a}, \tag{8.46}$$

where the third term on the r.h.s. is called the metric term.

When biharmonic viscosity is used (`VISBIHARM` option), the above operation is repeated twice using a viscosity coefficient ν_{BH}. The terms $\mathcal{V}_u$ and $\mathcal{V}_v$ given by (8.41) and (8.42) are sign-reversed and substituted as u and v in equations (8.39) and (8.40). A biharmonic scheme dissipates noise only on scales near the grid size. This scale selectivity allows the explicitly represented eddies to survive without unphysical damping in eddy-resolving models, although we must note that a biharmonic operator produces overshootings and spurious oscillations of variables (Delhez and Deleersnijder, 2007). A biharmonic viscosity scheme is not suitable for coarse resolution models that cannot resolve mesoscale eddies.

A non-slip condition is used for the side boundaries of topography by default in MRI.COM. A free-slip condition assuming zero viscosity there is also available.

8.3.2 Horizontal anisotropic viscosity (`VISANISO`)

Smith and McWilliams (2003) proposed a method of making a harmonic viscosity scheme anisotropic in an arbitrary direction. Setting σ_T and σ_S in equations (8.41) and (8.42) to

$$\begin{pmatrix} \sigma_T \\ \sigma_S \end{pmatrix} = \left[\begin{pmatrix} \frac{1}{2}(\nu_0+\nu_1) & 0 \\ 0 & \nu_1 \end{pmatrix} + (\nu_0-\nu_1) n_\mu n_\psi \begin{pmatrix} -2n_\mu n_\psi & n_\mu^2 - n_\psi^2 \\ n_\mu^2 - n_\psi^2 & 2n_\mu n_\psi \end{pmatrix} \right] \begin{pmatrix} D_T \\ D_S \end{pmatrix}, \tag{8.47}$$

where $\hat{\mathbf{n}} = (n_\mu, n_\psi)$ is a unit vector in an arbitrary direction and ν_0 (ν_1) is the viscosity coefficient parallel (perpendicular) to $\hat{\mathbf{n}}$. When `VISANISO` option is selected, $\hat{\mathbf{n}}$ is set to the direction of local flow in MRI.COM. Given the harmonic viscosity only in the direction of flow ($\nu_1 = 0$), the numerical noise is erased while the swift currents and eddy structures are maintained.

The following is a note on usage. The behavior of this scheme is specified at run time by namelist `nml_visaniso` (Table 8.2). The ratio ν_1/ν_0 should be given by `cc0` (default value is 0.2). The ratio at the lateral boundary should be given by `cc1` (default value is 0.5). When the variable `flgvisequator` is set as a positive number in the namelist, the ratio ν_1/ν_0 is tapered linearly from `cc0` at the latitude `flgvisequator` (in degrees) to `vis_factor_equator` at the Equator. The ratio is not tapered when a negative number is set, and the default value of `flgvisequator` is -1.

Table8.2 Namelist `nml_visaniso` anisotropic horizontal viscosity

variable	units	description	usage
`cc0`	1	the factor of anisotropy in viscosity; perpendicular / parallel (ν_1/ν_0) to the flow	default = 0.2
`cc1`	1	the factor (ν_1/ν_0) at lateral boundary	default = 0.5
`figvisequator`	degree latitude	the factor is tapered toward the Equator; when |LAT| < `flgvisequator` [deg]	default = -1 (no tapering)
`vis_factor_equator`	1	the factor at Equator when `flgvisequator` > 0	default = 0.0

8.3.3 Smagorinsky parameterization for horizontal viscosity (SMAGOR option)

To give the necessary but minimum viscosity to reduce numerical noise, the viscosity coefficient is made proportional to the local deformation rate (SMAGOR option; Smagorinsky, 1963; Griffies and Hallberg, 2000). When this parameterization is used with the biharmonic scheme, the scale selectivity of the viscosity scheme becomes more effective.

Defining deformation rate $|D|$:

$$|D| = \sqrt{D_T^2 + D_S^2}, \tag{8.48}$$

the viscosity coefficients are set as follows:

$$\nu_H = \left(\frac{C\Delta_{\min}}{\pi}\right)^2 |D|, \tag{8.49}$$

$$\nu_{BH} = \frac{\Delta_{\min}^2}{8}\nu_H, \tag{8.50}$$

where C (smagor_scale) is a dimensionless scaling parameter set by considering numerical stability and $\Delta_{\min}$ is the smaller of the zonal and meridional grid widths.

The parameter C should be selected to satisfy the following conditions.

- Restriction of grid Reynolds number:

$$\nu_H > U\frac{\Delta_{\min}}{2}, \tag{8.51}$$

- Restriction on the width of the lateral boundary layer:

$$\nu_H > \beta\Delta_{\min}^3, \tag{8.52}$$

- CFL condition:

$$\nu_H < \frac{\Delta_{\min}^2}{2\Delta t}, \tag{8.53}$$

where $\beta = df/dy$ is the meridional gradient of the Coriolis parameter. Scaling the deformation rate $|D|$ by $U/\Delta_{\min}$ gives the condition for stability: $C > \pi/\sqrt{2} \approx 2.2$ from (8.51) (Griffies and Hallberg, 2000).

Behavior of this scheme at run time is specified by namelist nml_smagor, whose components are listed on Table 8.3.

Table8.3 Namelist nml_smagor for Smagorinsky parameterization of horizontal viscosity coefficient

variable	units	description	usage
smagor_scale	1	scaling factor coefficient	default = −1.0
smagor_diff_ratio	1	ratio for diffusivity to scaling factor of viscosity (valid only when SMAGHD is specified)	required
l_smagor_nonzero_bg	logical	Use background viscosity as given by nml_baroclinic_visc_horz (Table 8.4)	default = .false.

8.3.4 Discretization of the horizontal viscosity term

Using the notations

$$\delta_\mu A_{i,j} \equiv \frac{A_{i+\frac{1}{2},j} - A_{i-\frac{1}{2},j}}{\Delta\mu}, \quad \delta_\psi A_{i,j} \equiv \frac{A_{i,j+\frac{1}{2}} - A_{i,j-\frac{1}{2}}}{\Delta\psi},$$
$$\delta_i A_{i,j} \equiv A_{i+\frac{1}{2},j} - A_{i-\frac{1}{2},j}, \quad \delta_j A_{i,j} \equiv A_{i,j+\frac{1}{2}} - A_{i,j-\frac{1}{2}},$$

and

$$\overline{A_{i,j}}^{\mu} \equiv \frac{1}{2}(A_{i-\frac{1}{2},j} + A_{i+\frac{1}{2},j}), \quad \overline{A_{i,j}}^{\psi} \equiv \frac{1}{2}(A_{i,j-\frac{1}{2}} + A_{i,j+\frac{1}{2}}),$$

deformation rates are discretized as follows:

$$
\begin{aligned}
D_{T\,i,j} =& \frac{h_{\psi i,j}}{h_{\mu i,j}} \overline{\delta_\mu \left(\frac{u}{h_\psi} \right)_{i,j}}^{\psi} - \frac{h_{\mu i,j}}{h_{\psi i,j}} \overline{\delta_\psi \left(\frac{v}{h_\mu} \right)_{i,j}}^{\mu}, \\
D_{S\,i,j} =& \frac{h_{\psi i,j}}{h_{\mu i,j}} \overline{\delta_\mu \left(\frac{v}{h_\psi} \right)_{i,j}}^{\psi} + \frac{h_{\mu i,j}}{h_{\psi i,j}} \overline{\delta_\psi \left(\frac{u}{h_\mu} \right)_{i,j}}^{\mu}.
\end{aligned}
\tag{8.54}
$$

Horizontal viscosity forces of (8.41) and (8.42) are discretized as follows:

$$
\begin{aligned}
F_{x\,i+\frac{1}{2},j+\frac{1}{2}} =& \frac{1}{\Delta V_{i+\frac{1}{2},j+\frac{1}{2}}} \\
& \times \left[\frac{1}{h^2_{\psi i+\frac{1}{2},j+\frac{1}{2}}} \delta_i \left(\Delta y \Delta z h^2_\psi \overline{\nu_H D_T}^{\psi} \right)_{i+\frac{1}{2},j+\frac{1}{2}} + \frac{1}{h^2_{\mu\,i+\frac{1}{2},j+\frac{1}{2}}} \delta_j \left(\Delta x \Delta z h^2_\mu \overline{\nu_H D_S}^{\mu} \right)_{i+\frac{1}{2},j+\frac{1}{2}} \right], \\
F_{y\,i+\frac{1}{2},j+\frac{1}{2}} =& \frac{1}{\Delta V_{i+\frac{1}{2},j+\frac{1}{2}}} \\
& \times \left[\frac{1}{h^2_{\psi i+\frac{1}{2},j+\frac{1}{2}}} \delta_i \left(\Delta y \Delta z h^2_\psi \overline{\nu_H D_S}^{\psi} \right)_{i+\frac{1}{2},j+\frac{1}{2}} - \frac{1}{h^2_{\mu\,i+\frac{1}{2},j+\frac{1}{2}}} \delta_j \left(\Delta x \Delta z h^2_\mu \overline{\nu_H D_T}^{\mu} \right)_{i+\frac{1}{2},j+\frac{1}{2}} \right].
\end{aligned}
\tag{8.55}
$$

The non-slip condition at the side boundaries of topography is discretized as follows. When the grid point $(i - \frac{1}{2}, j + \frac{1}{2})$ is defined as a (vertically partial) land (Figure 8.7a), the velocity gradients at the wall are calculated as follows:

$$
\begin{aligned}
\left(\frac{\partial u}{\partial x} \right)_{i,j+\frac{1}{2}} =& \frac{u_{i+\frac{1}{2},j+\frac{1}{2}}}{\Delta x^-_{ij}}, \\
\left(\frac{\partial v}{\partial x} \right)_{i,j+\frac{1}{2}} =& \frac{v_{i+\frac{1}{2},j+\frac{1}{2}}}{\Delta x^-_{ij}},
\end{aligned}
\tag{8.56}
$$

where Δx^-_{ij} is the length between the points $(i, j + \frac{1}{2})$ and $(i + \frac{1}{2}, j + \frac{1}{2})$. The contribution of this wall to the force is:

$$
\begin{aligned}
F^W_{x\;i+\frac{1}{2},j+\frac{1}{2}} =& - \frac{1}{\Delta V_{i+\frac{1}{2},j+\frac{1}{2}} h^2_{\psi\,i+\frac{1}{2},j+\frac{1}{2}}} \Delta y_{i,j+\frac{1}{2}} \Delta \tilde{z}_{i,j+\frac{1}{2}} h^2_{\psi\,i-\frac{1}{2},j} \nu_{H\,i-\frac{1}{2},j} \frac{u_{i+\frac{1}{2},j+\frac{1}{2}}}{\Delta x^-_{i+\frac{1}{2},j+\frac{1}{2}}}, \\
F^W_{y\;i+\frac{1}{2},j+\frac{1}{2}} =& - \frac{1}{\Delta V_{i+\frac{1}{2},j+\frac{1}{2}} h^2_{\psi\,i+\frac{1}{2},j+\frac{1}{2}}} \Delta y_{i,j+\frac{1}{2}} \Delta \tilde{z}_{i,j+\frac{1}{2}} h^2_{\psi\,i-\frac{1}{2},j} \nu_{H\,i-\frac{1}{2},j} \frac{v_{i+\frac{1}{2},j+\frac{1}{2}}}{\Delta x^-_{i+\frac{1}{2},j+\frac{1}{2}}},
\end{aligned}
\tag{8.57}
$$

where $\Delta \tilde{z}_{i,j+\frac{1}{2}}$ is the wall height.

8.3.5 Vertical viscosity

Only the harmonic scheme is considered. The vertical momentum flux is assumed to be proportional to the vertical gradient of velocity. For the upper part of a U-cell at the $(k - \frac{1}{2})$th vertical level, the momentum flux (positive upward) is calculated as follows:

$$
- \left(\nu_v \frac{\partial u}{\partial z} \right)_{k-1} = -\nu_{v\,k-1} \frac{u_{k-\frac{3}{2}} - u_{k-\frac{1}{2}}}{\Delta z_{k-1}},
$$

where $\Delta z_{k-1} = (\Delta z_{k-\frac{3}{2}} + \Delta z_{k-\frac{1}{2}})/2$, $\Delta z_{k-\frac{1}{2}}$ is the thickness of the U-cell (dzu), and ν_v is the vertical viscosity coefficient. Similarly, the momentum flux in the lower part of the U-cell is calculated as follows:

$$
- \left(\nu_v \frac{\partial u}{\partial z} \right)_{k} = -\nu_{v\,k} \frac{u_{k-\frac{1}{2}} - u_{k+\frac{1}{2}}}{\Delta z_{k}},
$$

where $\nu_{v\,k}$ is set to zero if the $(k + \frac{1}{2})$th level is the solid Earth. The bottom friction is calculated independently (see the next subsection). Also note that the variations of the grid thickness due to the partial bottom cell and the undulation of the sea surface are not considered when evaluating fluxes for simplicity.

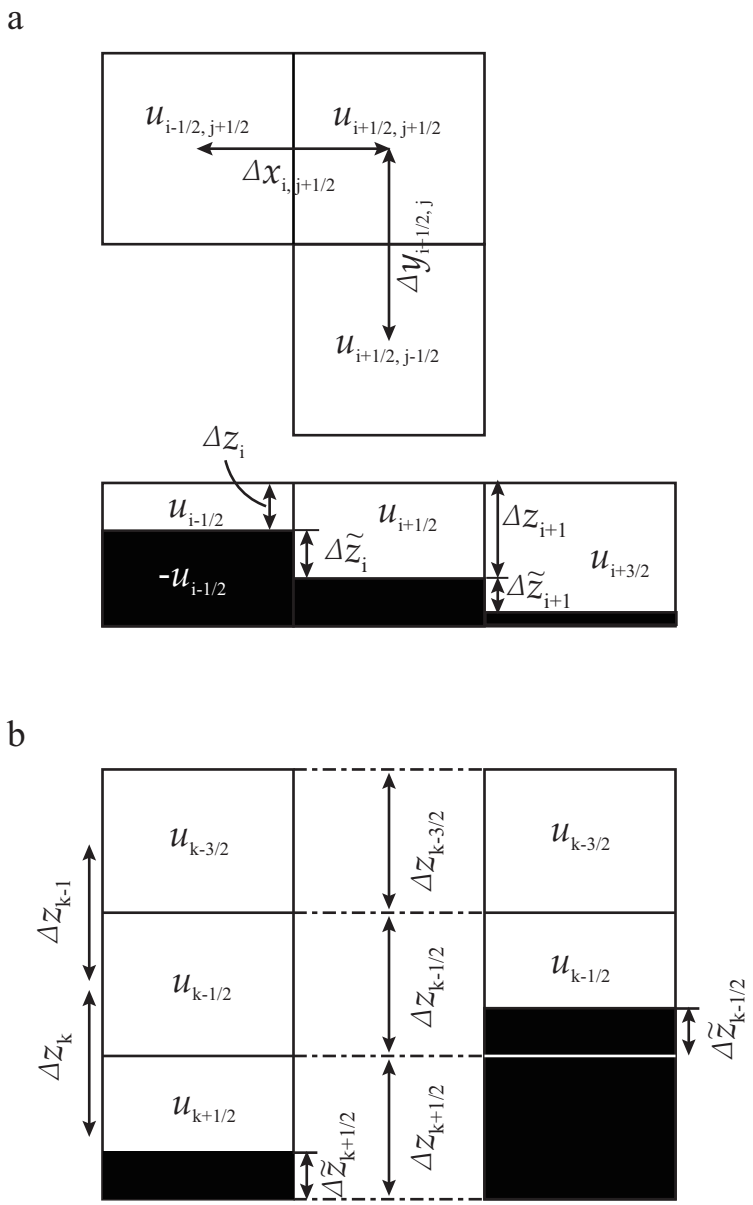

Figure8.7 (a) A schematic distribution of grids for horizontal viscosity. Upper: Plan view. Lower: Side view. The shadings denote solid earth. (b) A schematic distribution of grids for vertical viscosity. Side views. Left: The lower adjacent layer ($k + \frac{1}{2}$) has a sea bed. Right: The U-cell ($k - \frac{1}{2}$) has a sea bed.

To calculate viscosity, the divergence of the momentum flux is first calculated. The expression for the vertical viscosity term is

$$\frac{\partial}{\partial z}\left(\nu_v \frac{\partial u}{\partial z}\right)_{k-\frac{1}{2}} = \frac{\left(\nu_v \frac{\partial u}{\partial z}\right)_{k-1} - \left(\nu_v \frac{\partial u}{\partial z}\right)_k}{\widehat{\Delta z}_{k-\frac{1}{2}}} = \frac{\nu_{v\,k-1}(u_{k-\frac{3}{2}} - u_{k-\frac{1}{2}})}{\Delta z_{k-1}\widehat{\Delta z}_{k-\frac{1}{2}}} - \frac{\nu_{v\,k}(u_{k-\frac{1}{2}} - u_{k+\frac{1}{2}})}{\Delta z_k \widehat{\Delta z}_{k-\frac{1}{2}}} \tag{8.58}$$

where the variation of the grid thickness for the U-cell due to the partial bottom cell is now taken into account and is represented by $\widehat{\Delta z}$, that is, $\widehat{\Delta z}_{k-\frac{1}{2}} = \Delta z_{k-\frac{1}{2}} - \widetilde{\Delta z}_{k-\frac{1}{2}}$ (Figure 8.7(b)). Note that the first term on the r.h.s. of equation (8.58) is set to zero in calculating the viscosity term for the vertical level of $\frac{1}{2}$ ($k = 1$). See section 14.1 for sea surface wind stress. For the vertical viscosity coefficient ν_v, MRI.COM uses the larger of the value predicted by a turbulent closure scheme and a background one.

8.3.6 Bottom friction

When a U-cell in the $(k-\frac{1}{2})$th layer contains solid earth (Figure 8.7(b) right), the stress from the lower boundary (τ_x^b, τ_y^b) is calculated following Weatherly (1972). The specific expression is as follows:

$$\begin{pmatrix} \tau_x^b \\ \tau_y^b \end{pmatrix} = -\rho_0 C_{\mathrm{btm}} \sqrt{u_{k-\frac{1}{2}}^2 + v_{k-\frac{1}{2}}^2} \begin{pmatrix} \cos\theta_0 & -\sin\theta_0 \\ \sin\theta_0 & \cos\theta_0 \end{pmatrix} \begin{pmatrix} u_{k-\frac{1}{2}} \\ v_{k-\frac{1}{2}} \end{pmatrix},$$

where C_{btm} is a dimensionless constant. Viscous stress at the lower boundary has a magnitude proportional to the square of the flow speed at the U-cell and an angle $(\theta_0 + \pi)$ relative to the flow direction.

In MRI.COM,

$$\begin{aligned} C_{\mathrm{btm}} &= 1.225 \times 10^{-3} \\ \theta_0 &= \pm\pi/18 \quad \mathrm{rad} \qquad (\equiv 10^\circ), \end{aligned}$$

where θ_0 is positive (negative) in the northern (southern) hemisphere. This value of C_{btm} is based on previous research about the ratio of the friction velocity, u^*, to the geostrophic current velocity in the internal region, V_g, (specifically, 0.035 is used after the median value of the range reported in Section 4a of Weatherly (1972)), and the relation equation, $C_{\mathrm{btm}} = (u^*/V_g)^2$. The variables are designated in the model as C_{btm} = `abtm`, $\cos\theta_0$ = `bcs`, and $\sin(\pm\theta_0)$ = `isgn` $*$ `bsn`, where `isgn` = 1 in the northern hemisphere and `isgn` = −1 in the southern hemisphere.

8.4 Coriolis term

Because MRI.COM employs Arakawa B-grid arrangement, both of the horizontal components of velocity are defined at the same point. Coriolis term is evaluated by using the middle time level for the leap-frog scheme and the start time level for the Euler-backward scheme.

8.5 Usage

Runtime behavior of the baroclinic mode in the default settings is specified by the five namelist blocks (some of them are optional) shown on Tables 8.4 through 8.8. For the initial condition of the 3D velocity field, restart file must be prepared for X- and Y-ward velocities.

In addition, following model options are available.

`BIHARMONIC` or `VISBIHARM`: Biharmonic horizontal viscosity is used instead of harmonic viscosity
Specify `visc_horz_cm4ps` [$\mathrm{cm}^4\mathrm{sec}^{-1}$] instead of `visc_horz_cm2ps` [$\mathrm{cm}^2\mathrm{sec}^{-1}$] in namelist `nml_baroclinic_visc_horz`. See Section 8.3.1 for detail.

`VISANISO`: Anisotropic viscosity coefficients are used
Specify the coefficients by `nml_visaniso` (Table 8.2). See Section 8.3.2 for detail.

`SMAGOR` or `SMAGHD`: Smagorinsky parameterization is used for horizontal viscosity
Specify `nml_smagor` (Table 8.3) for factors of the Smagorinsky parameterization. See Section 8.3.3 for detail.

`VIS9P`: Nine points are used in computing viscosity
Five points are used by default.

See `docs/README.Namelist` for namelist details.

Table8.4 Namelist `nml_baroclinic_visc_horz` (required) for the horizontal viscosity (see Section 8.5)

variable	units	description	usage
`visc_horz_cm2ps`	$\mathrm{cm}^2\,\mathrm{sec}^{-1}$	horizontal viscosity (ν_H in Section 8.3.1)	required

Continued on next page

Table 8.4 – continued from previous page

variable	units	description	usage
`file_visc_horz_2d`	$cm^2\ sec^{-1}$	2D distribution of viscosity	optional (This overwrites `visc_horz_cm2ps`.)
`slip_factor`	factor	0.d0 means no-slip condition, while 1.d0 slip (Section 8.3.1)	default = 0.d0 (only valid with `VIS9P` option)

Table8.5 Namelist `nml_visc_vert_bg` (optional) for vertical viscosity (see Section 8.5)

variable	units	description	usage
`visc_vert_bg_cm2ps`	$cm^2\ sec^{-1}$	background vertical viscosity (ν_v in Section 8.3.5)	default = 1.d0

Table8.6 Namelist `nml_bottom_friction` (optional) for the bottom friction (see Section 8.5)

variable	units	description	usage
`btmfrc_scale`	1	$C_{\rm btm}$ in Section 8.3.6	default = 1.225d−3
`btmfrc_angle_deg`	degree	θ_0	default = 1.d1
`file_btm_frc_2d`	file name	2D distribution of $C_{\rm btm}$	optional (This overwrites `btmfrc_scale`)

Table8.7 Namelist `nml_hvisc_add` (optional) for additional horizonta viscosity (see Section 8.5)

variable	units	description	usage
`l_hvisc_add_harmonic`	logical	use additional harmonic viscosity or not	default = `.false.`
`file_hvisc_harmonic`	$cm^2\ sec^{-1}$	2D distribution of viscosity	file name

Table8.8 Namelist `nml_baroclinic_run` (optional) for starting the baroclinic mode (see Section 8.5)

variable	units	description	usage
`l_rst_baroclinic_in`	logical	read initial restart for 3D velocity or not	default = `l_rst_in`